NASA Technical Memorandum 84914

NASA-TM-84914 19850007404

F-8 Refueling Boom Ground Vibration Test

Michael W. Kehoe

January 1985

NASA
National Aeronautics and
Space Administration

9 1 1 RN/NASA-TM-84914
DISPLAY 09/6/1
85N15713*# ISSUE 7 PAGE 902 CATEGORY 5 RPT#: NASA-TM-84914 H-1194
NAS 1.15:84914 85/01/00 50 PAGES UNCLASSIFIED DOCUMENT
UTTL: F-8 refueling boom ground vibration test TLSP: Final Report
AUTH: A/KAHOE, M. W.
CORP: National Aeronautics and Space Administration. Ames Research Center, Moffett Field, Calif. AVAIL.NTIS SAP: HC A03/MF A01
MAJS: /*BOOMS (EQUIPMENT)/*F-8 AIRCRAFT/*MODAL RESPONSE/*VIBRATION/*VIBRATION DAMPING/*VIBRATION TESTS
MINS: / DYNAMIC RESPONSE/ FINITE ELEMENT METHOD/ FREQUENCY MEASUREMENT/ NASTRAN/ REFUELING
ABA: Author

NASA Technical Memorandum 84914

F-8 Refueling Boom Ground Vibration Test

Michael W. Kehoe
NASA Ames Research Center, Dryden Flight Research Facility, Edwards, California 93523

1985

National Aeronautics and
Space Administration
Ames Research Center
Dryden Flight Research Facility
Edwards, California 93523

SUMMARY

A ground vibration test was conducted on a simulated refueling boom mounted on NASA Ames Research Center's Dryden Flight Research Facility's digital, fly-by-wire F-8 airplane. The ground vibration test was conducted to determine if the refueling boom modal frequencies were close to the airplane modal frequencies. The data presented in this report include modal frequencies, mode shape data, and structural damping coefficients.

INTRODUCTION

NASA Ames Research Center's Dryden Flight Research Facility's digital, fly-by-wire F-8 airplane was modified to incorporate a simulated refueling boom. The boom was mounted to the aircraft at three locations on the forward left side of the fuselage; it is shown attached to the airplane in figure 1. The refueling boom was constructed from aluminum tubing with a diameter of 11.43 cm (4.5 in) and a wall thickness of 0.635 cm (0.25 in). The refueling boom support structure was made from 4130 steel tubing with a diameter of 1.91 cm (0.75 in) and a wall thickness of 0.15 cm (0.06 in). The overall length of the boom was approximately 3.51 m (11.5 ft). The complete refueling boom assembly weighed approximately 27.22 kg (60 lb), including a 2.02-kg (4.46-lb) receptacle mounted in the tip of the boom.

A ground vibration test (GVT) was performed on the refueling boom to measure the boom frequencies below 100 Hz and to compare the boom frequencies with the airplane flexible mode frequencies.

Following the GVT, a vibration analysis of the refueling boom was performed using the NASTRAN (ref. 1) finite-element program. The analysis was not done before the GVT was run because of the short time between notification and test. The objective of the analysis was to compare the frequencies and mode shapes obtained from the GVT with those obtained from the NASTRAN program.

TEST APPROACH

Ground Vibration Test

The refueling boom and its supporting structure were excited in the vertical and lateral directions with an instrumented hammer (impact excitation). In the vertical direction, 31 different locations on the boom assembly were excited; because of physical constraints, only 21 different locations were excited for lateral excitation. The boom and support structure excitation locations are illustrated in figures 2 and 3. A single-axis piezoelectric accelerometer was attached to the tip of the refueling boom (fig. 2) to measure the response of the boom resulting from the impact excitation.

Data were acquired for each impact location with a digital-computer-based structural analysis system. Transfer and coherence functions were then calculated. Five averages were used in each transfer-function calculation. Each impact location transfer and coherence function was reviewed to assess measurement quality before the functions were stored on the system disk. Frequency, damping, phase, and amplitude

were estimated for each structural mode by fitting a multidegree-of-freedom curve to a selected transfer function that exhibited a good response for the structural modes of interest. The estimated modal parameters, particularly phase, for each mode were examined to determine if the curve fit was acceptable. It was necessary to use several different transfer functions to ensure a good curve fit for all of the structural modes below 100 Hz.

After a good fit had been obtained for each structural mode of interest, a least-squared-error circle was fitted to the frequency-response data displayed in the Argand plane at each excitation coordinate to determine the modal coefficients. Once the modal coefficients were calculated, animated mode-shape displays were obtained.

Vibration Analysis

A NASTRAN finite-element model consisting of beam elements was used to represent the refueling boom and its supporting structure. The model of the refueling boom is illustrated in figure 4. It should be noted that the refueling boom assembly was constructed without engineering drawings; therefore, all of the dimensions used to create the NASTRAN model were obtained from measurements made with the boom installed on the aircraft.

RESULTS

Ground Vibration Test

Vertical Excitation. – The frequency-response functions obtained at locations 14 and 29 on the refueling boom are shown in figures 5 and 6. These two functions were sufficient to ensure a good curve fit for all of the structural modes below 100 Hz. The frequency-response function at location 14 on the boom had a bandwidth of 4.04 to 43.0 Hz. This bandwidth contained the first and second boom structural modes (fig. 7). Note that the first peak is split in the frequency range of 13 to 14 Hz. The response-function curve fit is shown in figure 8. Modal parameter estimates were extracted for each peak. The phase and amplitude estimates clearly indicated that only one valid mode was in the frequency range of 13 to 14 Hz. The estimated frequency, damping, and phase values for the first mode are presented in table 1.

The frequency-response function at location 29 had a bandwidth of 20.5 to 100 Hz (fig. 9). The modes identified in this bandwidth for the curve-fitting process are shown in figure 10. An excellent fit was obtained; the estimated frequency, damping, and phase values for each mode identified are presented in table 1.

The mode shapes and rectilinear mode coefficients for each mode identified below 100 Hz are presented in figures 11 through 17.

Lateral Excitation. – The frequency-response functions obtained for locations 15, 29, and 17 on the boom are shown in figures 18 through 20, respectively. Three response functions were required to obtain a good curve fit of the lateral modes excited below 100 Hz. A bandwidth from 4.40 to 44.6 Hz was used to isolate the first and second boom modes (fig. 21). Note that the 13-Hz peak is split. A good fit was obtained (fig. 22); the estimated modal parameters for the first mode (frequency, damping, and phase) are presented in table 2.

The frequency-response function at location 29 with a bandwidth of 15 to 96.9 Hz was used to estimate the modal parameters for all other modes below 100 Hz, except for a 70-Hz mode. The modes identified for the curve-fitting process are shown in figure 23. An excellent curve fit was obtained (fig. 24) for this response function. However, the estimated modal parameters extracted for the 63.7-Hz mode were poor. Several other frequency-response functions were examined, but a good response could not be obtained for lateral excitation, thus indicating that this was a mode with primarily vertical motion. The modal parameters estimated for the frequency-response function are presented in table 2.

The frequency-response function at location 17 with a bandwidth of 17.5 to 83 Hz was used primarily to identify the 70.74-Hz mode. The modes selected for the curve-fitting process are shown in figure 25. A good fit was obtained (fig. 26), and the estimated modal parameters for this mode are presented in table 2.

The mode shapes and rectilinear modal coefficients for each mode identified below 100 Hz are presented in figures 27 through 33.

Since the refueling boom was supported asymmetrically (fig. 3), each mode shape contained vertical and lateral motion regardless of the direction of the excitation. Therefore, the modes excited vertically and laterally had virtually the same frequency and damping (compare table 1 with table 2) with the exception of the 63.67-Hz and 70.69-Hz modes, which were excited primarily by vertical and lateral excitation, respectively.

Aircraft Modes. – A comparison of the boom natural frequencies with the aircraft structural frequencies is presented in table 3. The aircraft modal data were obtained from the Ling-Tempco-Vought (LTV) Corporation. The data in table 3 indicated that the boom modes of vibration were sufficiently separated from the airplane structural modes to avoid modal coupling. The 13.35-Hz boom mode and the 14.5-Hz vertical tail/fuselage torsion mode were the pair of modes with the smallest separation. The coupling of these two modes is unlikely since most of the motion of the 14.5-Hz vertical tail/fuselage torsion mode was in the aft fuselage area.

The aircraft was flown with the refueling boom and no adverse vibrations were revealed.

Vibration Analysis

A comparison of the NASTRAN finite-element analysis with the GVT results is presented in table 4. The predicted frequencies agreed well with the GVT results, with the exception of the second and fourth modes. The finite-element model was adjusted to obtain a better agreement between test and analysis. It was found that the inertia of the connections of the support rods to the refueling boom had the most significant effect on the modal frequencies. By adjusting the inertia, the second and fourth modal frequencies could be changed to agree more closely with the GVT results. However, by doing so, the error between the analytical and GVT frequencies of the other modes increased. It should again be noted that the finite-element model was not constructed from engineering drawings; all measurements were obtained while the boom was on the airplane.

The analytical mode shapes and modal coefficients are presented in figures 34 through 41. A comparison of the analytical and measured mode shapes indicated that

there was excellent agreement for the first three modes. Fair agreement was exhibited for the remainder of the modes. The largest discrepancy in these mode shapes was with the forward support rods.

CONCLUSIONS

A ground vibration test was conducted on a simulated refueling boom mounted on the ARC/DFRF digital, fly-by-wire F-8 airplane. Eight refueling boom modes below 100 Hz were identified. The refueling boom modes were sufficiently separated from the airplane flexible modes to prevent adverse coupling. The airplane was flown with the refueling boom and no adverse vibrations were detected.

A vibration analysis using the NASTRAN finite-element program was performed after the ground vibration test. All eight refueling boom modes were identified by the analysis.

Ames Research Center
Dryden Flight Research Facility
National Aeronautics and Space Administration
Edwards, California 93523, April 11, 1983

REFERENCE

1. The NASTRAN User's Manual (Level 17.0). NASA SP-222(04), 1979.

TABLE 1. — ESTIMATED MODAL PARAMETERS FOR VERTICAL EXCITATION

Frequency, Hz	Structural damping coefficient	Phase between force and response, deg	Response-function location
13.36	0.053	102.6	14
25.16	0.023	92.0	29
46.92	0.017	-94.5	29
49.83	0.01	-88.1	29
54.95	0.007	92.8	29
63.67	0.014	84.0	29
83.23	0.03	91.7	29

TABLE 2. — ESTIMATED MODAL PARAMETERS FOR LATERAL EXCITATION

Frequency, Hz	Structural damping coefficient	Phase between force and response, deg	Response-function location
13.50	0.045	90.0	15
25.10	0.026	87.4	29
46.74	0.020	-73.0	29
49.82	0.010	-92.0	29
54.90	0.009	-87.9	29
70.69	0.029	-91.7	17
82.41	0.036	92.3	29

TABLE 3. — REFUELING BOOM AND AIRPLANE MODES

(a) Refueling boom	
Mode	Frequency, Hz
Vertical	13.36
	25.16
	46.92
	49.83
	54.95
	63.67
Lateral	70.69
Vertical	83.23

(b) Airplane	
Mode	Frequency, Hz
Symmetric —	
Wing bending	8.1
Wing/fuselage	10.5
Horizontal tail bending	18.8
Wing/horizontal tail	22.6
Horizontal tail	32.6
Antisymmetric —	
Wing bending	8.1
Vertical tail bending fuselage torsion	11.1
Vertical tail bending fuselage torsion	14.5
Fuselage lateral bending/wing	17.7
Horizontal tail/vertical tail	19.2
Horizontal tail/vertical tail	22.4

TABLE 4. — COMPARISON OF GVT AND VIBRATION ANALYSIS RESULTS FROM VERTICAL EXCITATION

GVT, Hz	Analysis, Hz	Error, percent
13.36	13.26	-0.80
25.16	20.11	-20.10
46.92	46.67	-0.50
49.83	57.23	14.90
54.95	58.26	6.00
63.67	62.81	-1.40
70.69[a]	73.85	4.50
83.23	86.10	3.50

[a]Result from lateral excitation

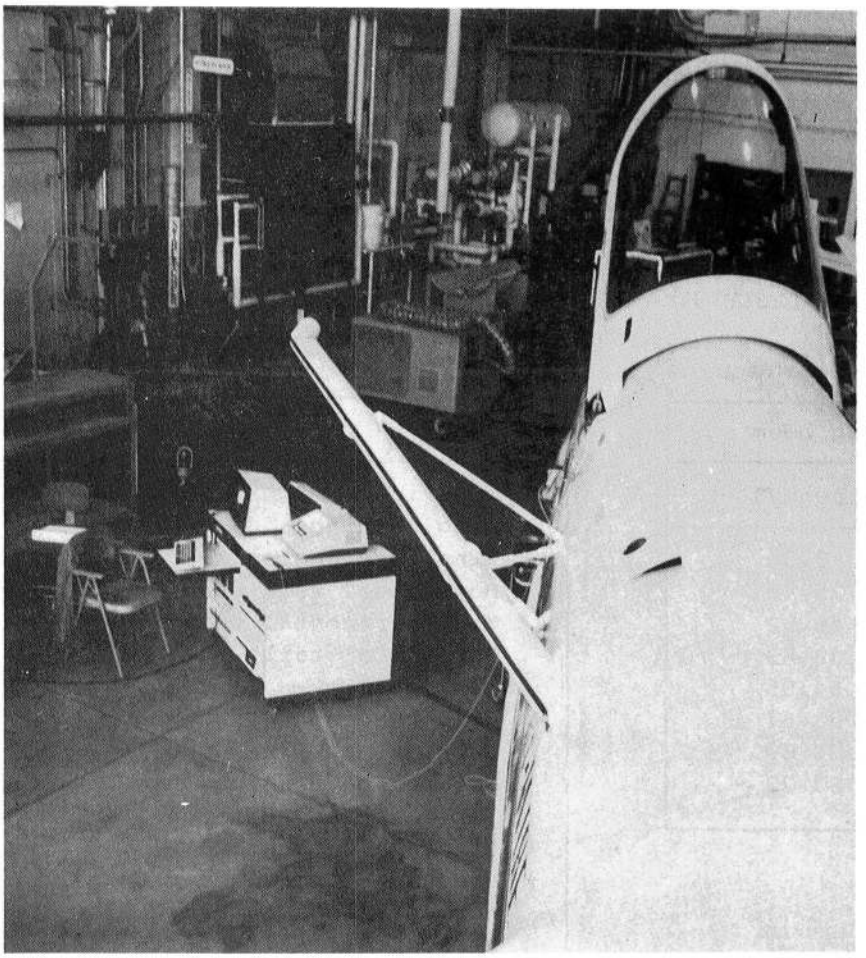

ECN 18088

Figure 1. F-8 airplane with simulated refueling boom.

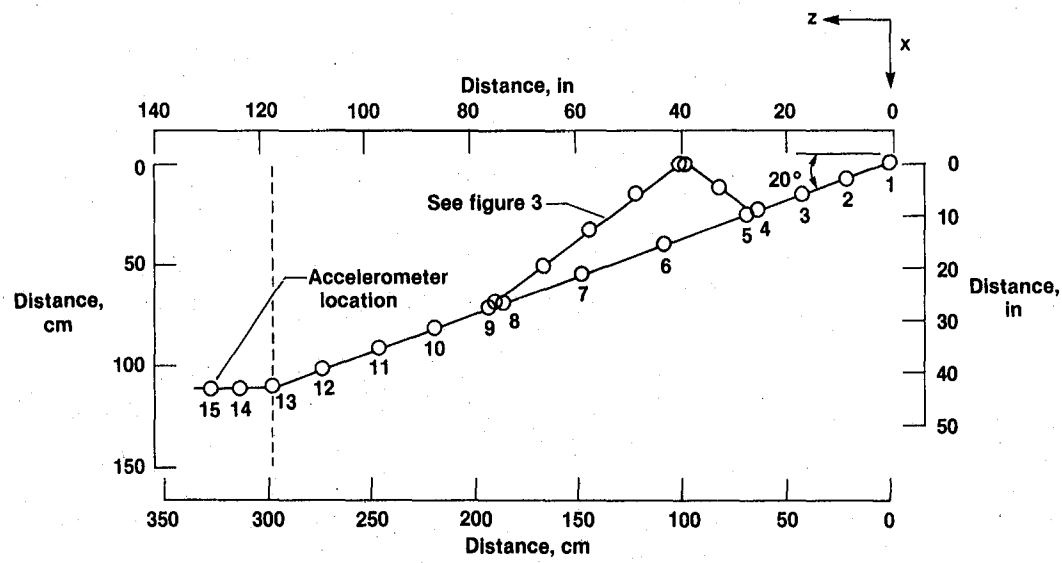

Point	x, cm (in)	y, cm (in)	z, cm (in)
1	0 (0)	0 (0)	0 (0)
2	8.38 (3.3)	0 (0)	21.34 (8.4)
3	16.51 (6.5)	0 (0)	42.67 (16.8)
4	24.89 (9.8)	0 (0)	64.01 (25.2)
5	26.67 (10.5)	0 (0)	68.58 (27.0)
6	41.91 (16.5)	0 (0)	107.70 (42.4)
7	57.15 (22.5)	0 (0)	146.81 (57.8)
8	72.39 (28.5)	0 (0)	185.67 (73.1)
9	74.42 (29.3)	0 (0)	191.01 (75.2)
10	84.58 (33.3)	0 (0)	217.17 (85.5)
11	94.74 (37.3)	0 (0)	243.33 (95.8)
12	104.90 (41.3)	0 (0)	269.24 (106.0)
13	115.06 (45.3)	0 (0)	295.40 (116.3)
14	115.06 (45.3)	0 (0)	310.64 (122.3)
15	115.06 (45.3)	0 (0)	328.42 (129.3)

Figure 2. Refueling boom excitation locations.

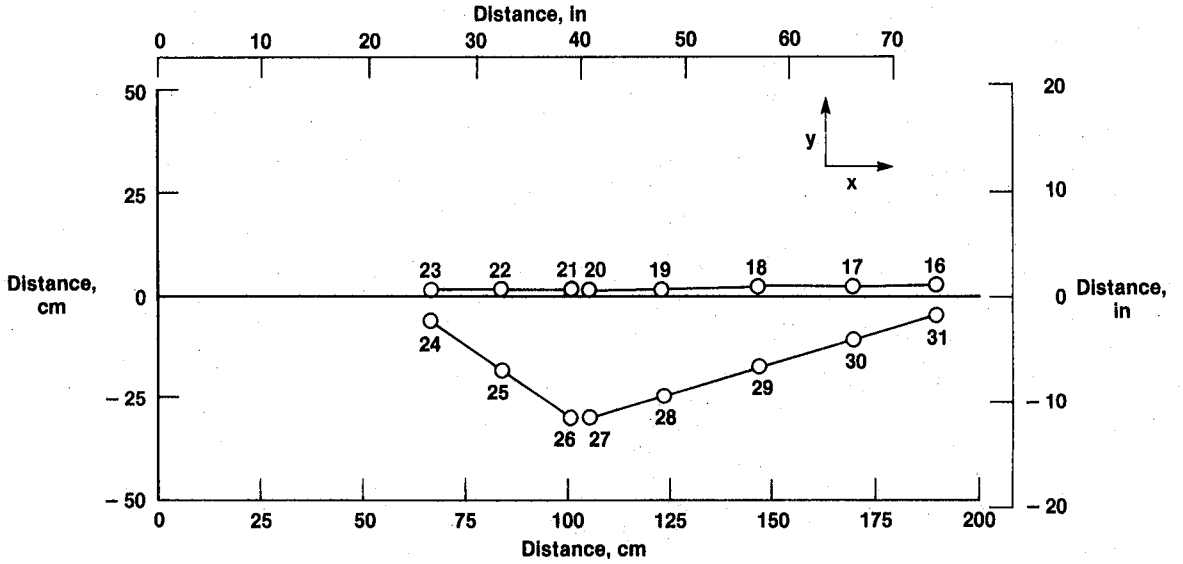

Point	x, cm (in)	y, cm (in)	z, cm (in)
16	68.58 (27.00)	2.54 (1.00)	188.21 (74.1)
17	52.07 (20.50)	2.24 (0.88)	167.64 (66.0)
18	32.77 (12.90)	1.88 (0.74)	144.78 (57.0)
19	14.99 (5.90)	1.55 (0.61)	121.92 (48.0)
20	0 (0)	1.27 (0.50)	104.14 (41.0)
21	0 (0)	1.27 (0.50)	99.06 (39.0)
22	9.86 (3.88)	1.27 (0.50)	82.55 (32.5)
23	19.69 (7.75)	1.27 (0.50)	66.04 (26.0)
24	25.40 (10.00)	-5.72 (-2.25)	66.04 (26.0)
25	12.70 (5.00)	-17.48 (-6.88)	82.55 (32.5)
26	0 (0)	-29.21 (-11.50)	99.06 (39.0)
27	0 (0)	-29.21 (-11.50)	104.14 (41.0)
28	14.76 (5.81)	-23.88 (-9.40)	121.92 (48.0)
29	33.78 (13.30)	-17.27 (-6.80)	144.78 (57.0)
30	52.83 (20.80)	-10.41 (-4.10)	167.64 (66.0)
31	69.85 (27.50)	-4.45 (-1.75)	188.21 (74.1)

Figure 3. Refueling boom support rod excitation location.

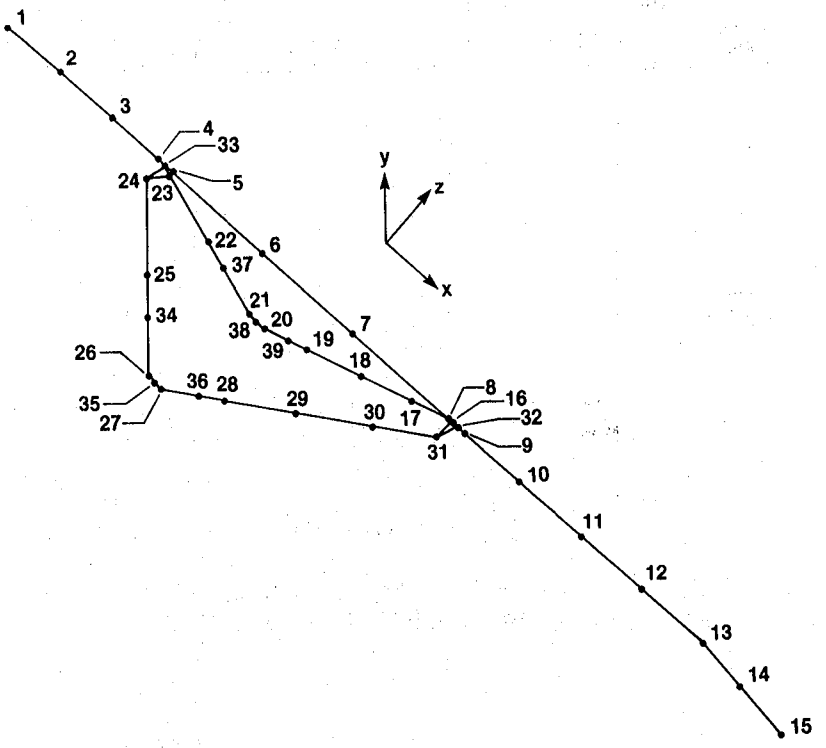

Figure 4. Finite-element model of the refueling boom assembly.

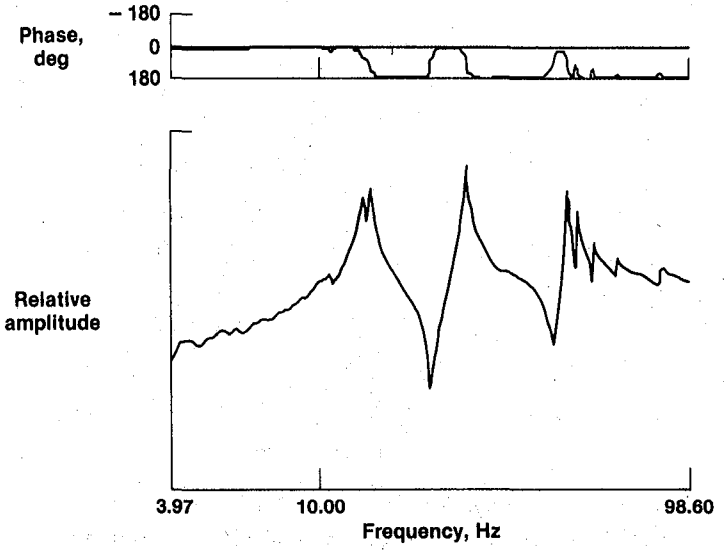

Figure 5. Frequency-response function at location 14 (vertical excitation).

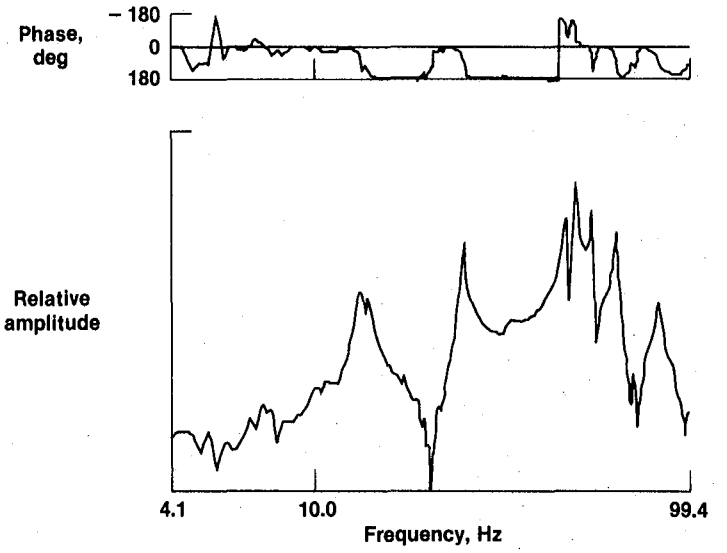

Figure 6. Frequency-response function at location 29 (vertical excitation).

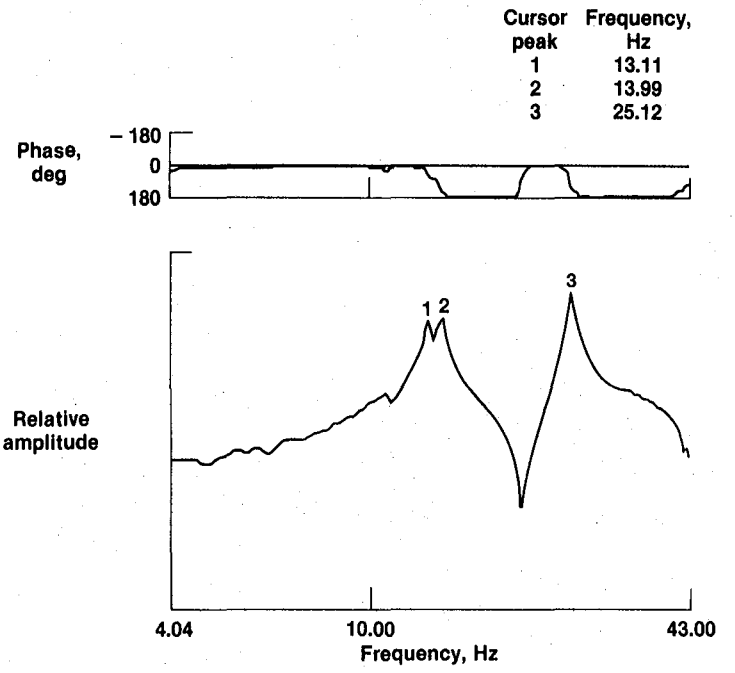

Figure 7. Expanded frequency-response function at location 14 (vertical excitation).

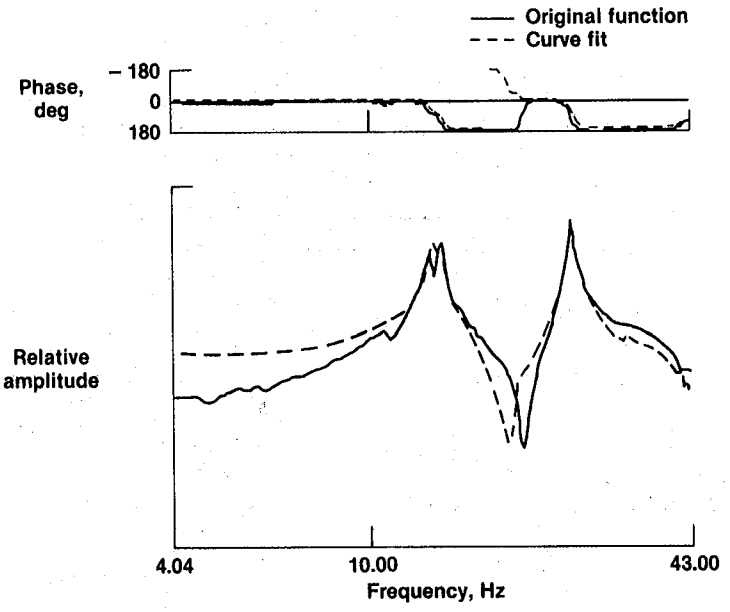

Figure 8. Curve fit to expanded frequency-response function at location 14 (vertical excitation).

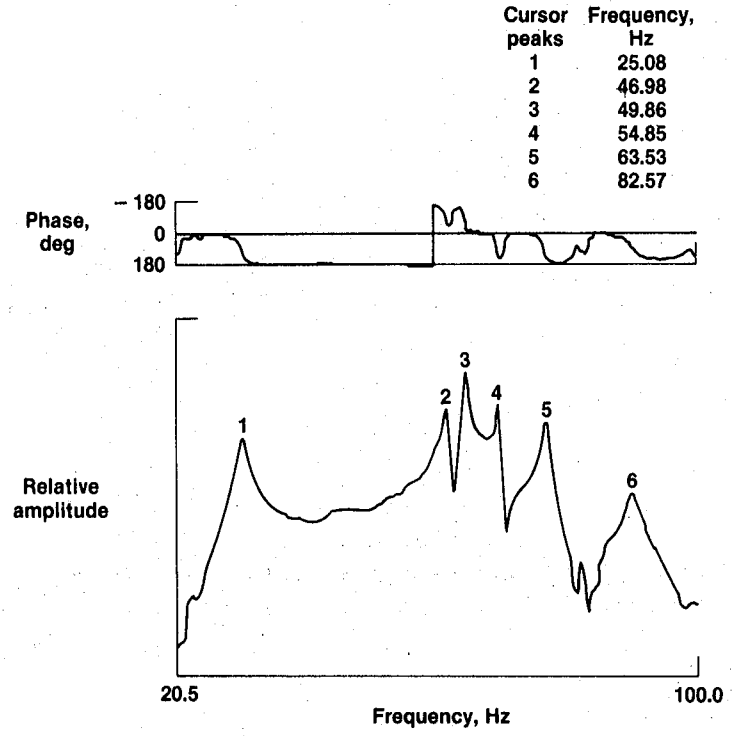

Figure 9. Expanded frequency-response function at location 29 (vertical excitation).

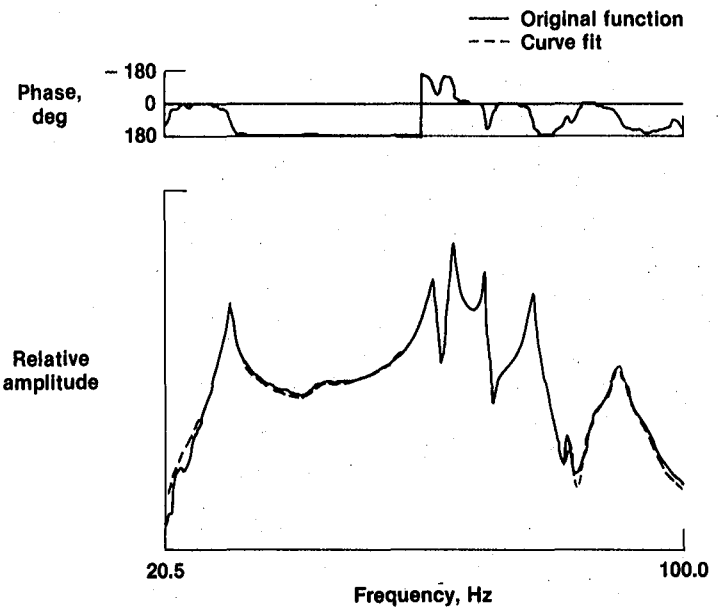

Figure 10. Curve fit to expanded frequency-response function at location 29 (vertical excitation).

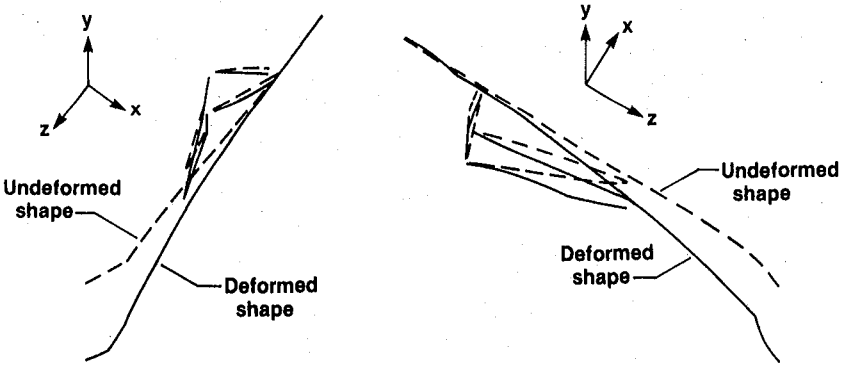

Figure 11. First mode of refueling boom assembly: vertical excitation frequency = 13.36 Hz, structural damping = 0.053.

Mode shape location	Coefficient x	y	z
1	0	-6.29	0
2	0	-12.45	0
3	0	-19.21	0
4	0	-22.00	0
5	0	-28.83	0
6	0	-52.50	0
7	0	-82.19	0
8	0	-124.35	0
9	0	-147.80	0
10	0	-184.68	0
11	0	-257.57	0
12	0	-316.98	0
13	0	-402.89	0
14	0	-494.48	0
15	0	-479.07	0
16	24.02	-136.30	0
17	19.90	-125.68	0
18	10.92	-89.05	0
19	-4.94	47.15	0
20	0.81	-9.34	0
21	1.13	-13.02	0
22	1.67	-19.31	0
23	2.45	-28.11	0
24	-12.54	-29.53	0
25	-22.83	-8.75	0
26	-84.50	3.93	0
27	-11.86	5.52	0
28	-47.86	3.33	0
29	-76.38	-30.86	0
30	-74.45	-85.65	0
31	-5.22	-149.88	0

Figure 11. Concluded.

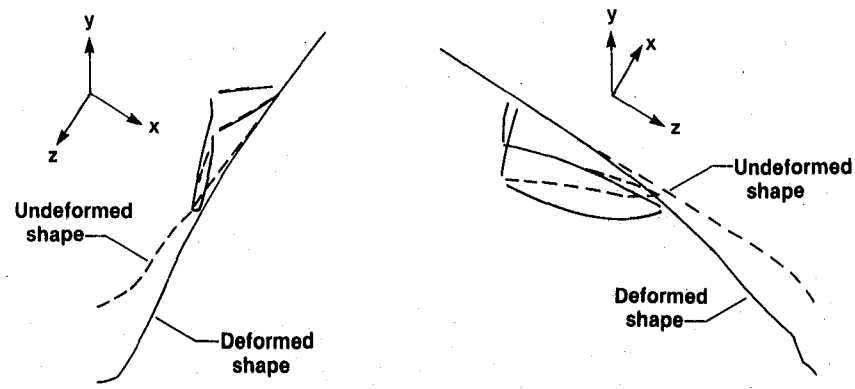

Mode shape location	Coefficient x	y	z
1	0	-7.99	0
2	0	-11.09	0
3	0	-7.82	0
4	0	-7.70	0
5	0	-9.11	0
6	0	-7.73	0
7	0	-42.21	0
8	0	-125.13	0
9	0	-147.33	0
10	0	-234.01	0
11	0	-378.72	0
12	0	-525.70	0
13	0	-611.84	0
14	0	-765.54	0
15	0	-704.70	0
16	10.81	-123.71	0
17	11.84	-36.49	0
18	7.49	-13.01	0
19	6.47	-7.70	0
20	6.16	-4.32	0
21	8.34	-5.84	0
22	2.19	-4.71	0
23	0.23	-2.75	0
24	0.51	-6.09	0
25	0.56	-8.13	0
26	-3.59	-1.30	0
27	-51.02	-18.57	0
28	-155.72	-109.04	0
29	-149.90	-214.08	0
30	-87.56	-240.62	0
31	-11.47	-131.23	0

Figure 12. Second mode of refueling boom assembly: vertical excitation frequency = 25.16 Hz, structural damping = 0.023.

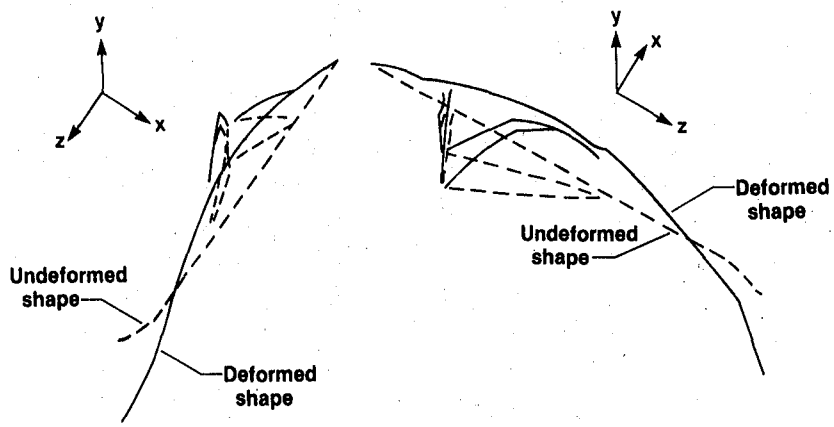

Mode shape location	Coefficient x	y	z
1	0	9.78	0
2	0	74.57	0
3	0	122.04	0
4	0	190.15	0
5	0	218.42	0
6	0	327.31	0
7	0	371.67	0
8	0	338.21	0
9	0	347.46	0
10	0	241.12	0
11	0	103.80	0
12	0	-73.13	0
13	0	-266.16	0
14	0	-428.71	0
15	0	-581.92	0
16	-153.90	266.62	0
17	-188.80	370.57	0
18	-150.76	392.82	0
19	-57.59	177.38	0
20	-1.79	6.74	0
21	-5.25	19.66	0
22	-26.63	99.48	0
23	-41.94	156.67	0
24	193.81	74.37	0
25	-77.23	-151.58	0
26	-14.47	54.04	0
27	-3.81	14.27	0
28	-258.26	54.87	0
29	-200.43	-450.24	0
30	425.21	-276.14	0
31	40.474	385.18	0

Figure 13. Third mode of refueling boom assembly: vertical excitation frequency = 46.92 Hz, structural damping = 0.017.

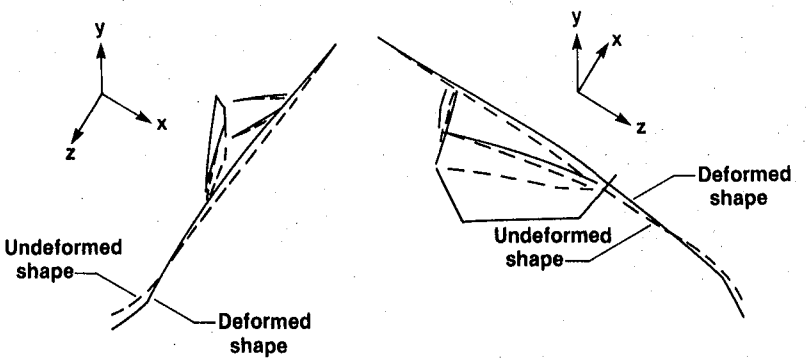

Mode shape location	Coefficient x	y	z
1	0	3.09	0
2	0	15.75	0
3	0	31.14	0
4	0	56.26	0
5	0	70.27	0
6	0	133.09	0
7	0	189.43	0
8	0	181.21	0
9	0	177.30	0
10	0	122.67	0
11	0	56.50	0
12	0	-25.56	0
13	0	-113.75	0
14	0	-195.87	0
15	0	-239.63	0
16	-56.99	156.62	0
17	-57.97	178.48	0
18	-29.02	116.48	0
19	-16.77	79.10	0
20	-2.97	17.05	0
21	-2.15	12.45	0
22	-6.26	35.78	0
23	-9.48	54.14	0
24	41.07	39.69	0
25	41.36	-45.96	0
26	-16.52	-13.92	0
27	-52.31	-43.88	0
28	-121.85	-867.22	0
29	999.41	-1035.00	0
30	1174.30	165.01	0
31	20.60	295.37	0

Figure 14. Fourth mode of refueling boom assembly: vertical excitation frequency = 49.83 Hz, structural damping = 0.01.

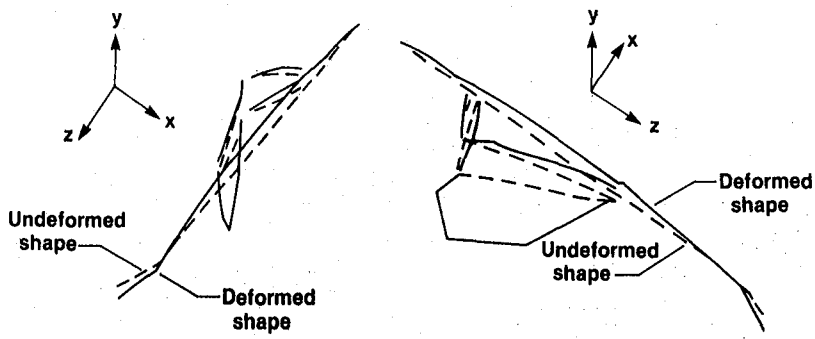

Mode shape location	Coefficient x	y	z
1	0	4.49	0
2	0	28.70	0
3	0	43.10	0
4	0	67.75	0
5	0	76.49	0
6	0	108.98	0
7	0	116.74	0
8	0	105.97	0
9	0	108.90	0
10	0	80.86	0
11	0	48.70	0
12	0	7.76	0
13	0	-37.12	0
14	0	-70.25	0
15	0	-104.20	0
16	-18.18	103.23	0
17	-17.90	113.06	0
18	-10.52	85.71	0
19	-6.23	59.37	0
20	-0.89	10.42	0
21	-0.78	9.04	0
22	-3.58	41.07	0
23	-5.29	60.75	0
24	31.33	73.86	0
25	56.46	21.67	0
26	18.52	-8.63	0
27	-24.39	11.37	0
28	-383.67	26.82	0
29	-566.70	-228.96	0
30	-277.23	-318.92	0
31	1.84	53.08	0

Figure 15. Fifth mode of refueling boom assembly: vertical excitation frequency = 54.95 Hz, structural damping = 0.007.

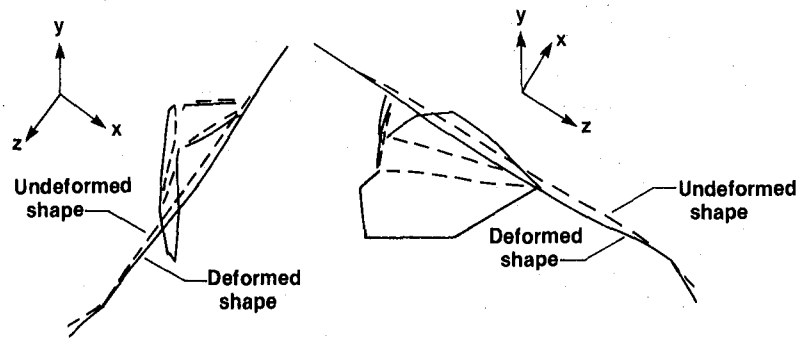

Mode shape location	Coefficient x	y	z
1	0	-1.60	0
2	0	-11.96	0
3	0	-19.16	0
4	0	-29.74	0
5	0	-33.48	0
6	0	-49.63	0
7	0	-59.82	0
8	0	-55.63	0
9	0	-55.31	0
10	0	-44.45	0
11	0	-30.99	0
12	0	-11.70	0
13	0	-9.08	0
14	0	-30.30	0
15	0	-54.94	0
16	8.19	-46.50	0
17	-25.40	160.43	0
18	-27.42	223.45	0
19	-14.01	133.38	0
20	1.71	-19.62	0
21	-0.26	3.13	0
22	0.88	-10.27	0
23	1.85	-21.25	0
24	-10.33	-24.36	0
25	-22.27	-8.54	0
26	-11.21	5.22	0
27	-12.80	5.96	0
28	-229.17	16.02	0
29	-364.27	-147.17	0
30	-185.62	-213.55	0
31	0.20	5.89	0

Figure 16. Sixth mode of refueling boom assembly: vertical excitation frequency = 63.67 Hz, structural damping = 0.014.

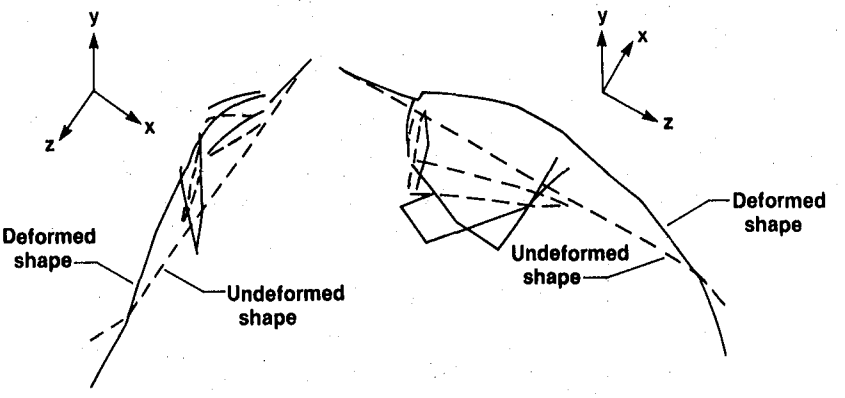

Mode shape location	Coefficient x	y	z
1	0	-1.95	0
2	0	1.55	0
3	0	5.62	0
4	0	11.98	0
5	0	23.07	0
6	0	46.25	0
7	0	65.36	0
8	0	64.37	0
9	0	59.25	0
10	0	47.51	0
11	0	40.56	0
12	0	16.33	0
13	0	-7.234	0
14	0	-19.90	0
15	0	-43.90	0
16	-8.92	50.62	0
17	2.81	-17.80	0
18	9.13	-74.42	0
19	5.86	-55.80	0
20	0.81	-9.31	0
21	-0.90	10.40	0
22	-1.29	14.84	0
23	-1.58	18.14	0
24	4.80	11.32	0
25	13.17	5.05	0
26	5.71	-2.66	0
27	20.47	-9.54	0
28	-36.34	2.53	0
29	-49.65	-20.05	0
30	-3.07	-3.53	0
31	1.42	41.00	0

Figure 17. Eighth mode of refueling boom assembly: vertical excitation frequency = 83.23 Hz, structural damping = 0.03.

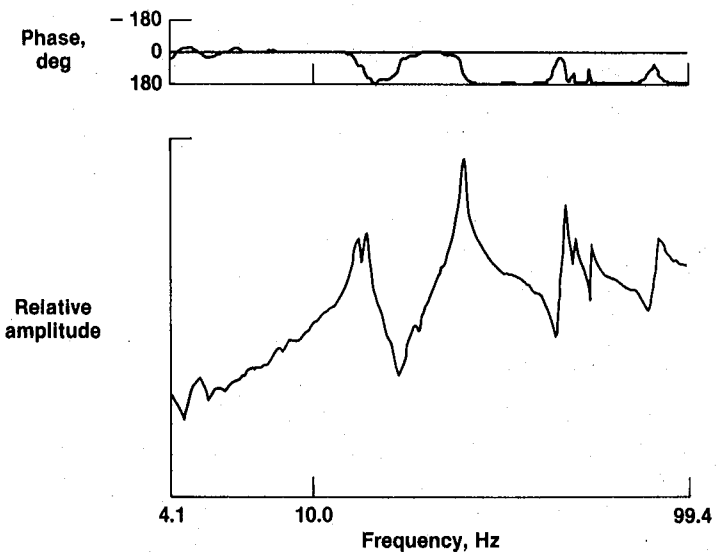

Figure 18. Frequency-response function at location 15 (lateral excitation).

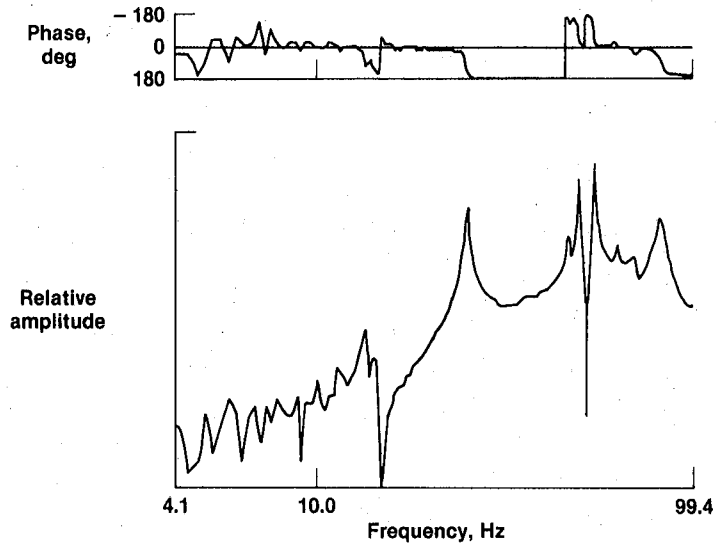

Figure 19. Frequency-response function at location 29 (lateral excitation).

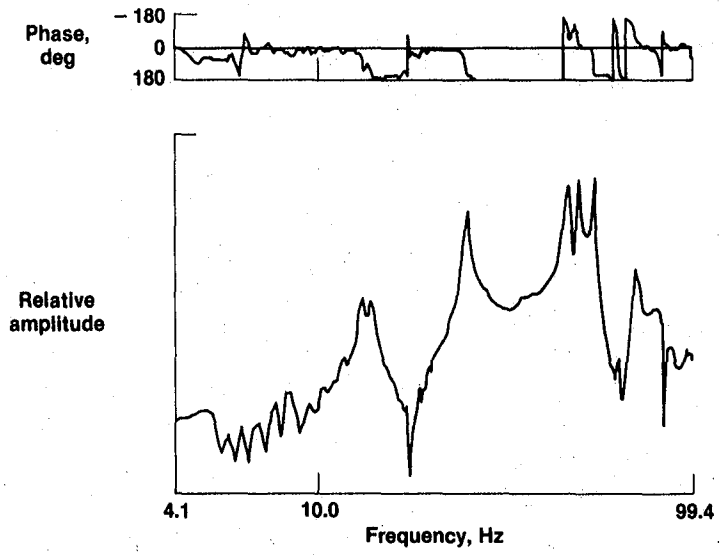

Figure 20. Frequency-response function at location 17 (lateral excitation).

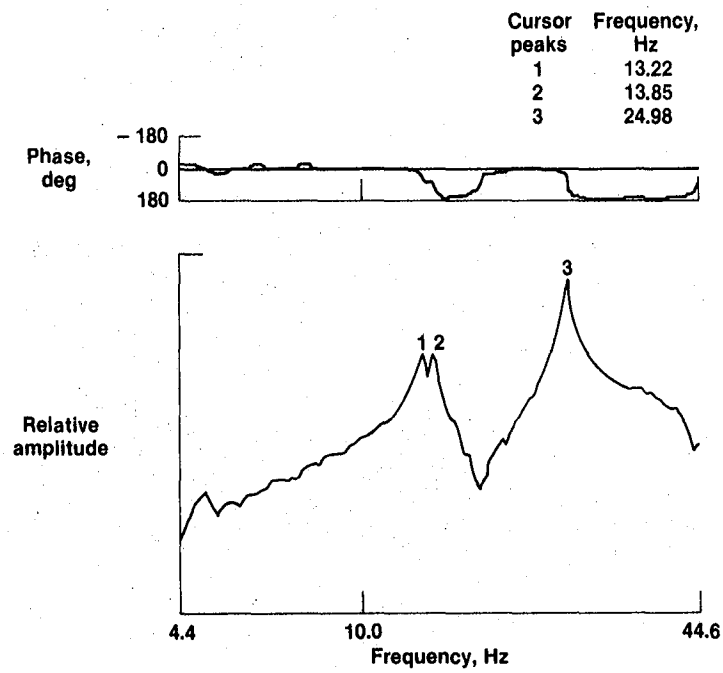

Figure 21. Expanded frequency-response function at location 15 (lateral excitation).

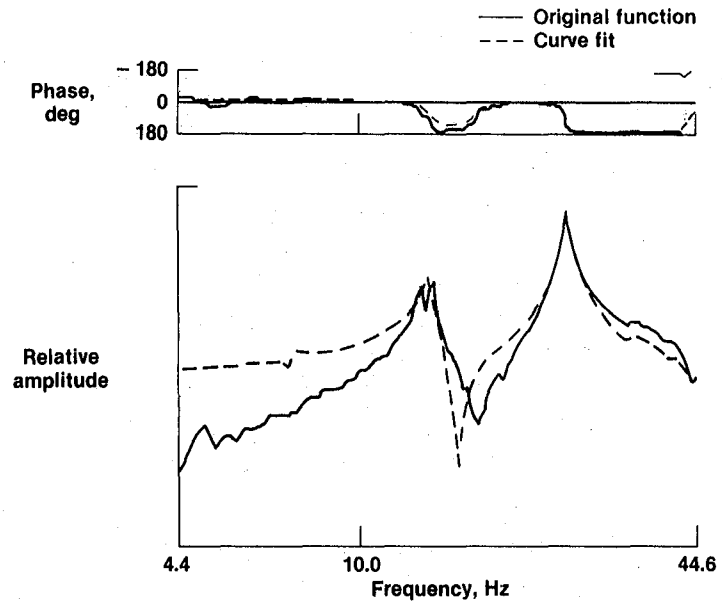

Figure 22. Curve fit to expanded frequency-response function at location 15 (lateral excitation).

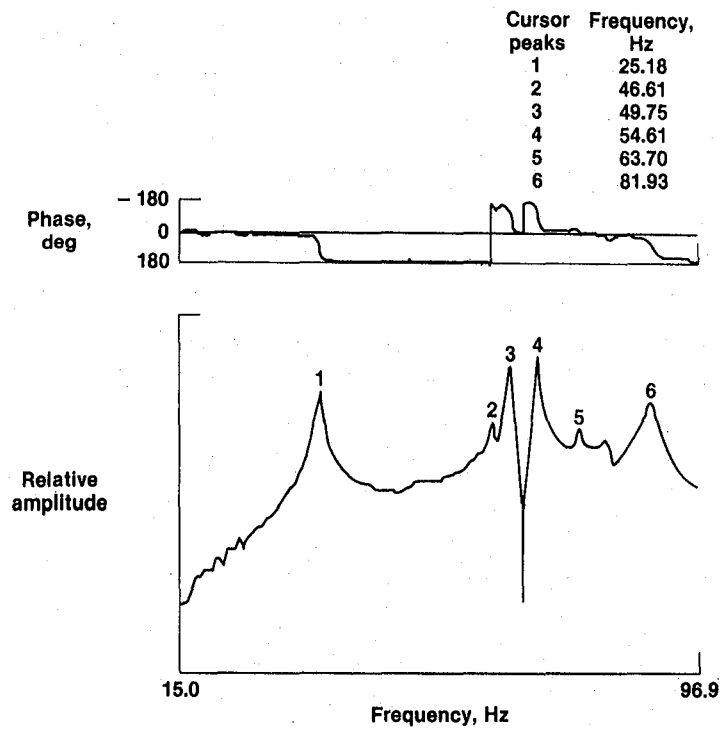

Figure 23. Expanded frequency-response function at location 29 (lateral excitation).

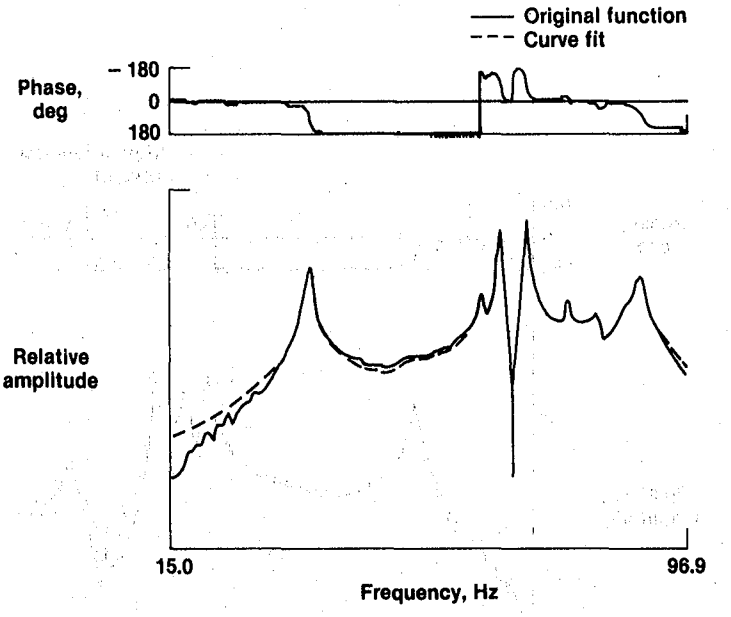

Figure 24. Curve fit to expanded frequency-response function at location 29 (lateral excitation).

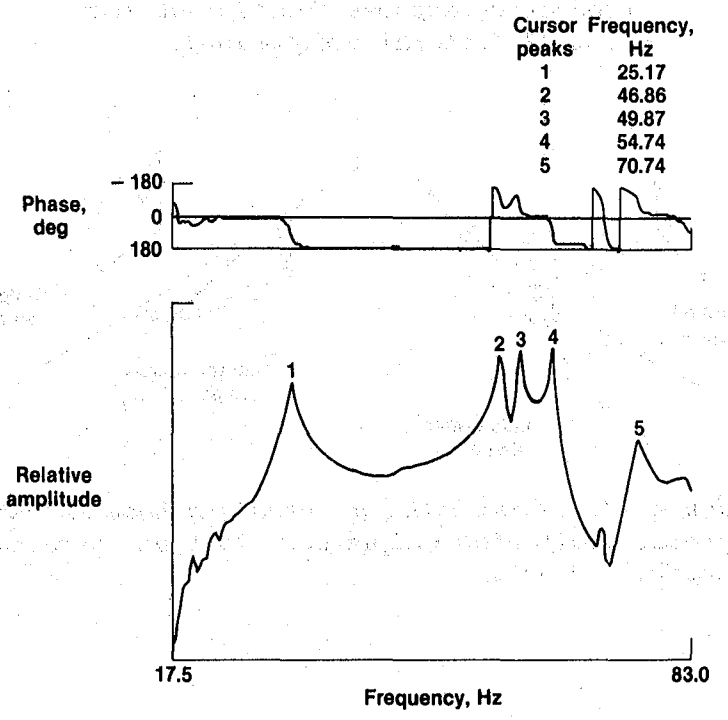

Figure 25. Expanded frequency-response function at location 17 (lateral excitation).

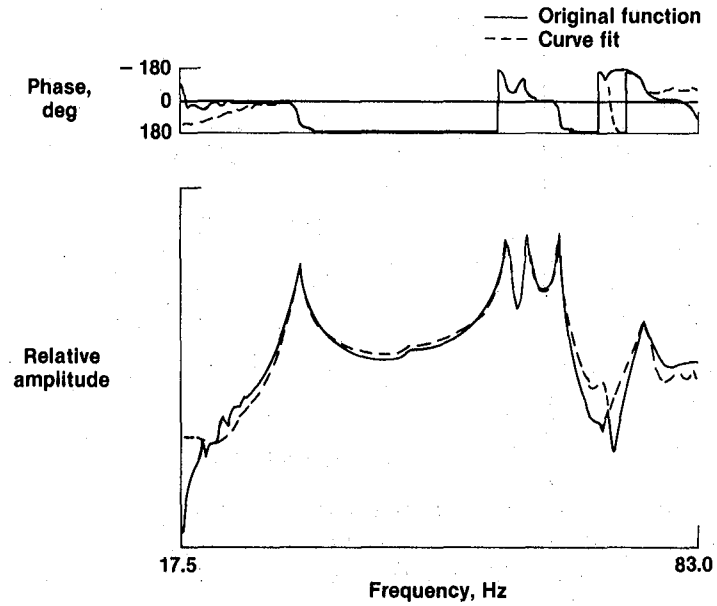

Figure 26. Curve fit to expanded frequency-response function at location 17 (lateral excitation).

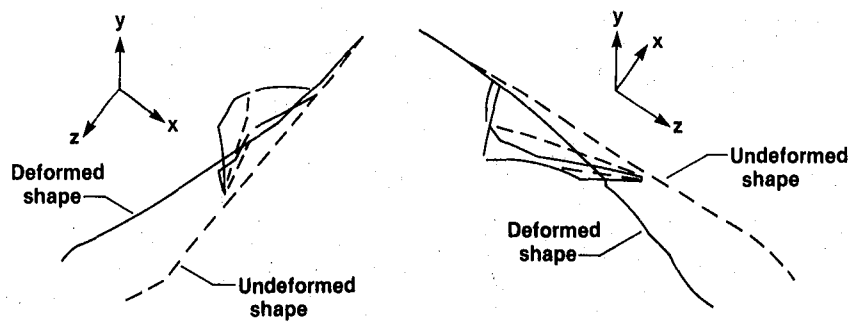

Figure 27. First mode of refueling boom assembly: lateral excitation frequency = 13.5 Hz, structural damping = 0.045.

Mode shape location	Coefficient x	y	z
1	-4.56	0	0
2	-3.55	0	0
3	-6.49	0	0
4	-9.54	0	0
5	-14.77	0	0
6	-28.84	0	0
7	-58.58	0	0
8	-84.85	0	0
9	-95.05	0	0
10	-115.16	0	0
11	-145.49	0	0
12	-168.64	0	0
13	-204.05	0	0
14	-205.89	0	0
15	-190.44	0	0
16	0	0	0
17	-31.38	-4.97	0
18	-64.18	-7.87	0
19	-47.65	-5.00	0
20	0	0	0
21	0	0	0
22	0	0	0
23	0	0	0
24	0	0	0
25	0	0	0
26	0	0	0
27	0	0	0
28	0.77	11.17	0
29	-3.85	9.55	0
30	-29.83	25.93	0
31	0	0	0

Figure 27. Concluded.

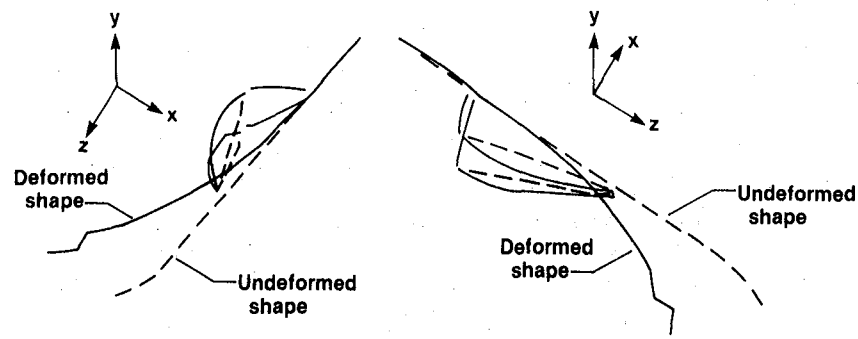

Mode shape location	Coefficient x	y	z
1	28.22	0	0
2	40.97	0	0
3	27.51	0	0
4	12.04	0	0
5	8.59	0	0
6	-18.72	0	0
7	-59.70	0	0
8	-210.58	0	0
9	-240.55	0	0
10	-416.54	0	0
11	-557.01	0	0
12	-740.58	0	0
13	-1056.10	0	0
14	-931.94	0	0
15	-1099.60	0	0
16	0	0	0
17	-272.90	-43.22	0
18	-281.29	-34.53	0
19	-185.85	-19.53	0
20	0	0	0
21	0	0	0
22	0	0	0
23	0	0	0
24	0	0	0
25	0	0	0
26	0	0	0
27	0	0	0
28	15.23	218.20	0
29	-104.30	258.20	0
30	-195.15	169.64	0
31	0	0	0

Figure 28. Second mode of refueling boom assembly: lateral excitation frequency = 25.1 Hz, structural damping = 0.026.

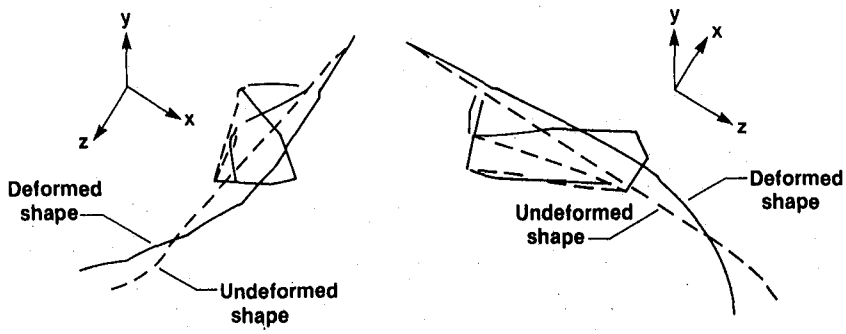

Mode shape location	Coefficient x	y	z
1	-6.37	0	0
2	32.90	0	0
3	67.00	0	0
4	100.63	0	0
5	132.97	0	0
6	186.16	0	0
7	261.51	0	0
8	252.26	0	0
9	245.49	0	0
10	167.47	0	0
11	67.98	0	0
12	-68.69	0	0
13	-225.69	0	0
14	-291.61	0	0
15	-352.12	0	0
16	0	0	0
17	511.36	80.98	0
18	759.73	93.27	0
19	524.93	55.13	0
20	0	0	0
21	0	0	0
22	0	0	0
23	0	0	0
24	0	0	0
25	0	0	0
26	0	0	0
27	0	0	0
28	3.43	49.10	0
29	25.13	-62.25	0
30	130.35	-113.31	0
31	0	0	0

Figure 29. Third mode of refueling boom assembly: lateral excitation frequency = 46.74 Hz, structural damping = 0.02.

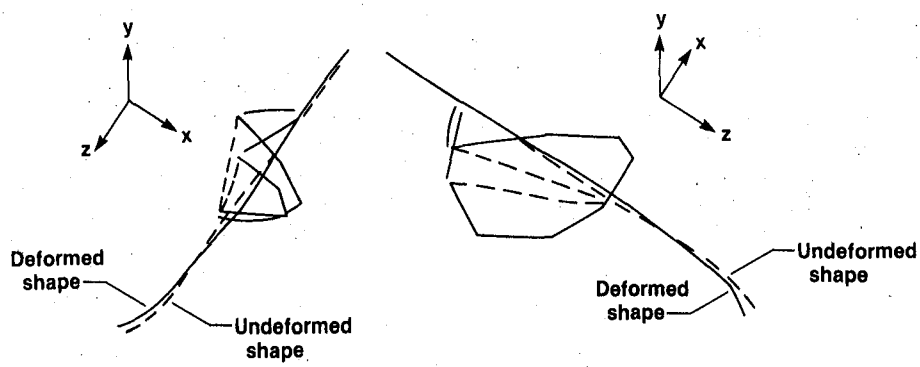

Mode shape location	Coefficient x	y	z
1	-3.84	0	0
2	-11.78	0	0
3	-13.85	0	0
4	-11.53	0	0
5	-12.76	0	0
6	16.51	0	0
7	34.86	0	0
8	48.02	0	0
9	39.31	0	0
10	33.75	0	0
11	8.73	0	0
12	-18.12	0	0
13	-54.73	0	0
14	-55.39	0	0
15	-88.13	0	0
16	0	0	0
17	566.80	89.76	0
18	763.23	93.70	0
19	501.51	52.68	0
20	0	0	0
21	0	0	0
22	0	0	0
23	0	0	0
24	0	0	0
25	0	0	0
26	0	0	0
27	0	0	0
28	-33.42	-478.36	0
29	228.43	-565.40	0
30	277.27	-241.03	0
31	0	0	0

Figure 30. Fourth mode of refueling boom assembly: lateral excitation frequency = 49.82 Hz, structural damping = 0.01.

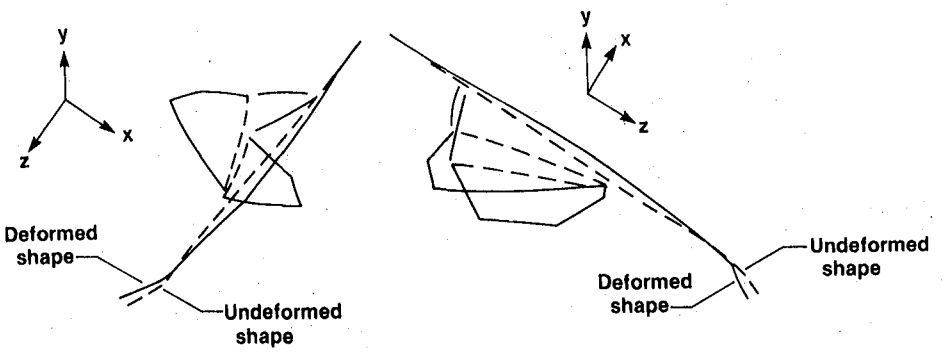

Mode shape location	Coefficient x	y	z
1	2.31	0	0
2	15.01	0	0
3	32.37	0	0
4	49.69	0	0
5	65.06	0	0
6	93.63	0	0
7	131.15	0	0
8	129.13	0	0
9	125.97	0	0
10	94.47	0	0
11	55.69	0	0
12	3.74	0	0
13	-54.44	0	0
14	-81.65	0	0
15	-109.87	0	0
16	0	0	0
17	-634.10	-100.42	0
18	-959.04	-117.75	0
19	-627.34	-65.91	0
20	0	0	0
21	0	0	0
22	0	0	0
23	0	0	0
24	0	0	0
25	0	0	0
26	0	0	0
27	0	0	0
28	-44.51	-637.06	0
29	321.87	-796.72	0
30	419.39	-364.57	0
31	0	0	0

Figure 31. Fifth mode of refueling boom assembly: lateral excitation frequency = 54.9 Hz, structural damping = 0.009.

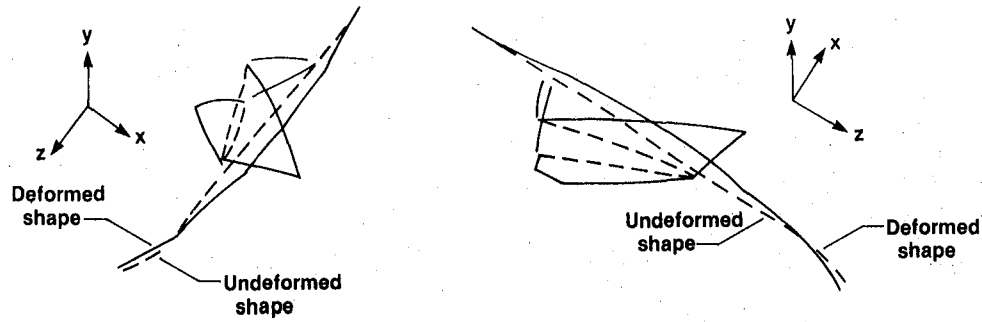

Mode shape location	Coefficient x	y	z
1	0.90	0	0
2	1.67	0	0
3	5.25	0	0
4	7.31	0	0
5	9.98	0	0
6	12.41	0	0
7	14.86	0	0
8	12.62	0	0
9	12.44	0	0
10	9.57	0	0
11	5.83	0	0
12	3.43	0	0
13	-4.82	0	0
14	-3.79	0	0
15	-5.14	0	0
16	0	0	0
17	62.53	9.90	0
18	45.38	5.56	0
19	26.23	2.75	0
20	0	0	0
21	0	0	0
22	0	0	0
23	0	0	0
24	0	0	0
25	0	0	0
26	0	0	0
27	0	0	0
28	1.76	25.21	0
29	-13.67	33.85	0
30	-17.02	14.80	0
31	0	0	0

Figure 32. Seventh mode of refueling boom assembly: lateral excitation frequency = 70.69 Hz, structural damping = 0.029.

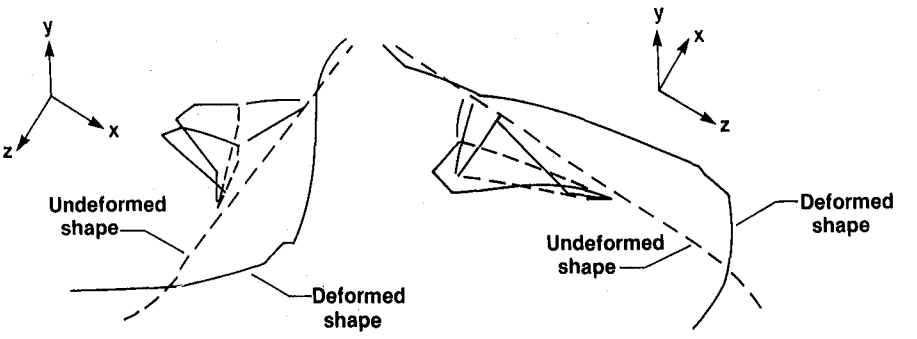

Mode shape location	Coefficient x	y	z
1	-17.85	0	0
2	-26.69	0	0
3	-11.10	0	0
4	14.87	0	0
5	28.38	0	0
6	96.08	0	0
7	143.91	0	0
8	174.84	0	0
9	162.81	0	0
10	157.06	0	0
11	101.03	0	0
12	37.99	0	0
13	-38.99	0	0
14	-76.74	0	0
15	-140.18	0	0
16	0	0	0
17	-25.43	-4.02	0
18	-152.90	-18.77	0
19	-117.87	-12.38	0
20	0	0	0
21	0	0	0
22	0	0	0
23	0	0	0
24	0	0	0
25	0	0	0
26	0	0	0
27	0	0	0
28	10.67	152.68	0
29	-72.75	180.08	0
30	-8.69	7.55	0
31	0	0	0

Figure 33. Eighth mode of refueling boom assembly: lateral excitation frequency = 82.41 Hz, structural damping = 0.036.

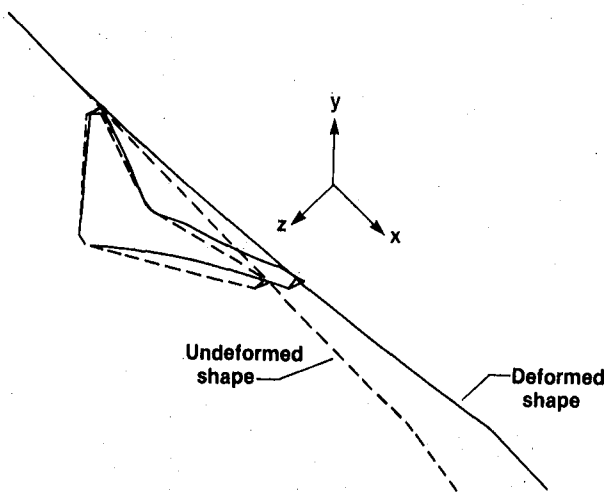

Point	Coefficient x	y	z
1	0	0	0
2	3.02×10^{-4}	3.71×10^{-3}	4.10×10^{-4}
3	1.51×10^{-3}	1.54×10^{-2}	3.21×10^{-3}
4	4.57×10^{-3}	3.60×10^{-2}	1.06×10^{-2}
5	5.55×10^{-3}	4.16×10^{-2}	1.30×10^{-2}
6	1.85×10^{-2}	1.07×10^{-1}	4.55×10^{-2}
7	3.97×10^{-2}	2.04×10^{-1}	9.89×10^{-2}
8	6.89×10^{-2}	3.29×10^{-1}	1.72×10^{-1}
9	7.33×10^{-2}	3.46×10^{-1}	1.84×10^{-1}
10	9.80×10^{-2}	4.54×10^{-1}	2.47×10^{-1}
11	1.25×10^{-1}	5.74×10^{-1}	3.19×10^{-1}

Figure 34. First boom mode predicted by NASTRAN: frequency = 13.26 Hz.

12	1.55×10^{-1}	7.02×10^{-1}	3.95×10^{-1}
13	1.86×10^{-1}	8.36×10^{-1}	4.75×10^{-1}
14	1.86×10^{-1}	9.11×10^{-1}	5.22×10^{-1}
15	1.86×10^{-1}	1.00	5.78×10^{-1}
16	9.25×10^{-2}	3.61×10^{-1}	1.65×10^{-1}
17	1.28×10^{-1}	3.83×10^{-1}	1.99×10^{-1}
18	1.21×10^{-1}	2.89×10^{-1}	1.78×10^{-1}
19	3.32×10^{-2}	1.24×10^{-1}	5.00×10^{-2}
20	-3.41×10^{-4}	2.89×10^{-3}	1.00×10^{-3}
21	8.03×10^{-5}	2.70×10^{-3}	3.47×10^{-4}
22	-5.36×10^{-3}	3.43×10^{-2}	1.11×10^{-2}
23	-4.77×10^{-3}	3.64×10^{-2}	1.21×10^{-2}
24	1.54×10^{-2}	3.83×10^{-2}	1.02×10^{-2}
25	1.90×10^{-2}	3.89×10^{-2}	7.18×10^{-3}
26	-2.86×10^{-5}	3.34×10^{-3}	-2.54×10^{-5}
27	2.36×10^{-4}	9.71×10^{-3}	-6.10×10^{-4}
28	-1.94×10^{-3}	1.62×10^{-1}	4.53×10^{-2}
29	3.11×10^{-2}	3.22×10^{-1}	1.33×10^{-1}
30	7.31×10^{-2}	3.86×10^{-1}	1.97×10^{-1}
31	8.84×10^{-2}	3.54×10^{-1}	1.96×10^{-1}
32	7.11×10^{-2}	3.38×10^{-1}	1.77×10^{-1}
33	4.84×10^{-3}	3.84×10^{-2}	1.16×10^{-2}
34	1.64×10^{-2}	3.00×10^{-2}	2.86×10^{-3}
35	0	0	0
36	-5.44×10^{-3}	9.31×10^{-2}	1.94×10^{-2}
37	-2.15×10^{-3}	2.52×10^{-2}	4.98×10^{-3}
38	0	0	0
39	1.52×10^{-2}	6.42×10^{-2}	2.43×10^{-2}

Figure 34. Concluded.

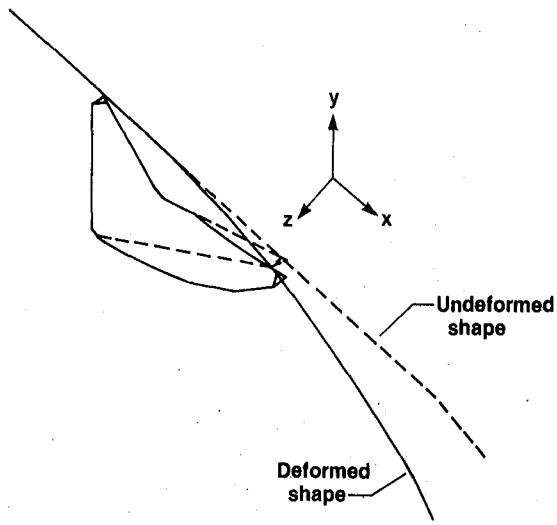

Point	Coefficient x	y	z
1	0	0	0
2	4.54×10^{-4}	7.32×10^{-4}	-1.44×10^{-3}
3	4.90×10^{-4}	1.99×10^{-3}	-4.00×10^{-3}
4	7.32×10^{-4}	2.52×10^{-3}	-5.98×10^{-3}
5	8.75×10^{-4}	2.40×10^{-3}	-6.17×10^{-3}
6	5.73×10^{-3}	-5.56×10^{-3}	1.73×10^{-3}
7	2.35×10^{-2}	-3.48×10^{-2}	4.29×10^{-2}
8	6.33×10^{-2}	-9.78×10^{-2}	1.39×10^{-1}
9	7.07×10^{-2}	-1.09×10^{-1}	1.58×10^{-1}
10	1.15×10^{-1}	-1.83×10^{-1}	2.75×10^{-1}
11	1.72×10^{-1}	-2.77×10^{-1}	4.21×10^{-1}

Figure 35. Second boom mode predicted by NASTRAN: frequency = 20.11 Hz.

12	2.37×10^{-1}	-3.83×10^{-1}	5.87×10^{-1}
13	3.07×10^{-1}	-4.97×10^{-1}	7.66×10^{-1}
14	3.07×10^{-1}	-5.63×10^{-1}	8.74×10^{-1}
15	3.07×10^{-1}	-6.39×10^{-1}	1.00
16	9.60×10^{-2}	-6.88×10^{-2}	1.30×10^{-1}
17	1.37×10^{-1}	-9.20×10^{-3}	1.80×10^{-1}
18	1.07×10^{-1}	2.99×10^{-2}	1.41×10^{-1}
19	3.11×10^{-2}	2.41×10^{-2}	3.97×10^{-2}
20	-1.08×10^{-4}	-7.55×10^{-4}	5.02×10^{-4}
21	-2.54×10^{-5}	-1.17×10^{-4}	-8.80×10^{-5}
22	2.35×10^{-3}	3.68×10^{-3}	-4.59×10^{-3}
23	2.86×10^{-3}	2.42×10^{-3}	-6.10×10^{-3}
24	4.31×10^{-3}	2.46×10^{-3}	-6.39×10^{-3}
25	5.18×10^{-3}	6.28×10^{-3}	-3.25×10^{-3}
26	-1.95×10^{-5}	1.74×10^{-3}	-9.79×10^{-5}
27	-4.09×10^{-4}	-1.70×10^{-2}	1.38×10^{-3}
28	9.73×10^{-2}	-7.99×10^{-2}	1.06×10^{-1}
29	2.07×10^{-1}	-9.66×10^{-2}	2.48×10^{-1}
30	2.17×10^{-1}	-9.09×10^{-2}	2.77×10^{-1}
31	1.19×10^{-1}	-7.78×10^{-2}	1.78×10^{-1}
32	6.70×10^{-2}	-1.03×10^{-1}	1.48×10^{-1}
33	7.98×10^{-4}	2.41×10^{-3}	-6.07×10^{-3}
34	4.57×10^{-3}	6.86×10^{-3}	-1.64×10^{-3}
35	0	0	0
36	5.02×10^{-2}	-6.93×10^{-2}	4.83×10^{-2}
37	1.45×10^{-3}	2.78×10^{-3}	-2.85×10^{-3}
38	0	0	0
39	1.26×10^{-2}	1.18×10^{-2}	1.75×10^{-2}

Figure 35. Concluded.

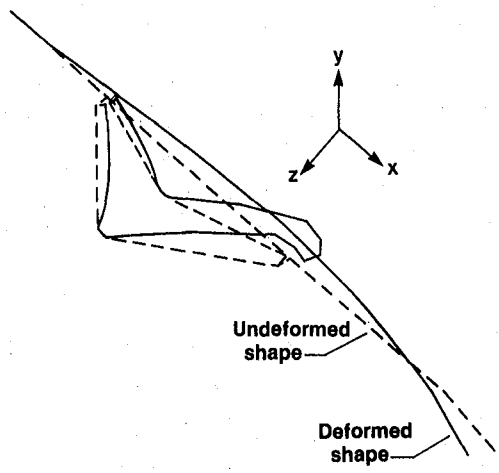

Point	Coefficient x	y	z
1	0	0	0
2	1.03×10^{-3}	1.41×10^{-2}	3.31×10^{-3}
3	4.77×10^{-3}	5.11×10^{-2}	1.37×10^{-2}
4	1.18×10^{-2}	1.03×10^{-1}	3.22×10^{-2}
5	1.37×10^{-2}	1.16×10^{-1}	3.73×10^{-2}
6	3.32×10^{-2}	2.24×10^{-1}	8.77×10^{-2}
7	4.88×10^{-2}	2.96×10^{-1}	1.28×10^{-1}
8	5.08×10^{-2}	2.91×10^{-1}	1.33×10^{-1}
9	4.97×10^{-2}	2.83×10^{-1}	1.30×10^{-1}
10	3.90×10^{-2}	2.22×10^{-1}	1.03×10^{-1}
11	2.08×10^{-2}	1.28×10^{-1}	5.62×10^{-2}

Figure 36. Third boom mode predicted by NASTRAN: frequency = 46.67 Hz.

12	-3.09×10^{-3}	8.49×10^{-3}	-4.83×10^{-3}
13	-3.07×10^{-2}	-1.29×10^{-1}	-7.62×10^{-2}
14	-3.03×10^{-2}	-2.05×10^{-1}	-1.20×10^{-1}
15	-3.08×10^{-2}	-2.95×10^{-1}	-1.72×10^{-1}
16	8.69×10^{-2}	3.10×10^{-1}	1.19×10^{-1}
17	2.05×10^{-1}	6.17×10^{-1}	2.72×10^{-1}
18	2.64×10^{-1}	8.15×10^{-1}	3.42×10^{-1}
19	1.42×10^{-1}	4.80×10^{-1}	1.77×10^{-1}
20	-6.48×10^{-5}	1.01×10^{-2}	4.62×10^{-4}
21	2.51×10^{-4}	7.55×10^{-3}	1.05×10^{-3}
22	-1.60×10^{-2}	9.35×10^{-2}	3.35×10^{-2}
23	-1.40×10^{-2}	1.00×10^{-1}	3.65×10^{-2}
24	4.33×10^{-2}	1.08×10^{-1}	2.74×10^{-2}
25	5.82×10^{-2}	1.15×10^{-1}	1.78×10^{-2}
26	-9.34×10^{-5}	1.08×10^{-2}	-1.50×10^{-4}
27	1.22×10^{-4}	1.80×10^{-2}	-1.42×10^{-4}
28	6.48×10^{-2}	6.06×10^{-1}	2.83×10^{-1}
29	1.25×10^{-1}	1.00	4.91×10^{-1}
30	1.04×10^{-1}	6.98×10^{-1}	3.54×10^{-1}
31	5.50×10^{-2}	3.03×10^{-1}	1.52×10^{-1}
32	5.03×10^{-2}	2.88×10^{-1}	1.32×10^{-1}
33	1.23×10^{-2}	1.09×10^{-1}	3.44×10^{-2}
34	5.18×10^{-2}	9.27×10^{-2}	6.63×10^{-3}
35	0	0	0
36	3.41×10^{-2}	3.54×10^{-1}	1.58×10^{-1}
37	-6.69×10^{-3}	6.91×10^{-2}	1.54×10^{-2}
38	0	0	0
39	7.34×10^{-2}	2.70×10^{-1}	9.61×10^{-2}

Figure 36. Concluded.

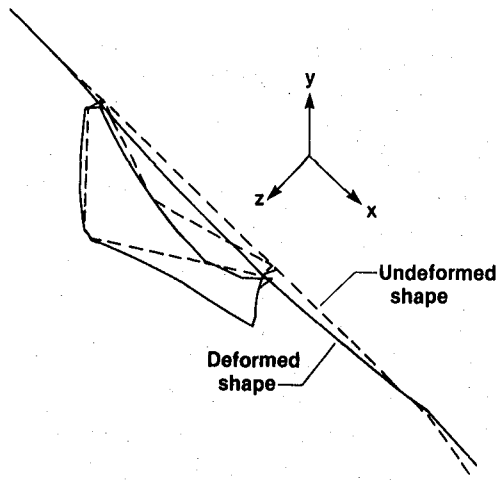

Point	Coefficient x	y	z
1	0	0	0
2	-1.93×10^{-4}	-5.21×10^{-3}	-6.26×10^{-4}
3	-1.59×10^{-4}	-1.92×10^{-2}	-6.46×10^{-4}
4	1.19×10^{-3}	-4.01×10^{-2}	2.67×10^{-3}
5	1.76×10^{-3}	-4.52×10^{-2}	4.07×10^{-3}
6	9.66×10^{-3}	-9.12×10^{-2}	2.35×10^{-2}
7	1.80×10^{-2}	-1.23×10^{-1}	4.43×10^{-2}
8	2.12×10^{-2}	-1.25×10^{-1}	5.16×10^{-2}
9	2.10×10^{-2}	-1.23×10^{-1}	5.10×10^{-2}
10	1.80×10^{-2}	-1.03×10^{-1}	4.33×10^{-2}
11	1.22×10^{-2}	-7.04×10^{-2}	2.64×10^{-2}

Figure 37. Fourth boom mode predicted by NASTRAN: frequency = 57.23 Hz.

12	4.18×10^{-3}	-2.67×10^{-2}	7.81×10^{-3}
13	-5.46×10^{-3}	2.53×10^{-2}	-1.70×10^{-2}
14	-5.46×10^{-3}	5.80×10^{-2}	-3.25×10^{-2}
15	-5.46×10^{-3}	9.69×10^{-2}	-5.18×10^{-2}
16	4.26×10^{-2}	-1.03×10^{-1}	4.04×10^{-2}
17	1.32×10^{-1}	-1.67×10^{-1}	1.54×10^{-1}
18	1.34×10^{-1}	-2.04×10^{-1}	1.58×10^{-1}
19	5.03×10^{-2}	-1.16×10^{-1}	5.47×10^{-2}
20	8.08×10^{-5}	-9.46×10^{-3}	2.84×10^{-4}
21	2.62×10^{-5}	-2.46×10^{-3}	2.86×10^{-5}
22	-3.35×10^{-3}	-4.91×10^{-2}	6.25×10^{-3}
23	-1.31×10^{-3}	-4.27×10^{-2}	3.46×10^{-3}
24	-2.09×10^{-2}	-4.23×10^{-2}	3.38×10^{-3}
25	-3.75×10^{-2}	-6.32×10^{-2}	2.28×10^{-3}
26	8.84×10^{-5}	-9.53×10^{-3}	3.30×10^{-4}
27	-1.30×10^{-4}	-1.47×10^{-2}	1.79×10^{-3}
28	3.42×10^{-1}	4.00×10^{-1}	5.65×10^{-1}
29	6.54×10^{-1}	5.58×10^{-1}	1.00
30	4.19×10^{-1}	1.54×10^{-1}	5.82×10^{-1}
31	6.63×10^{-2}	-1.09×10^{-1}	7.04×10^{-2}
32	2.11×10^{-2}	-1.24×10^{-1}	5.14×10^{-2}
33	1.34×10^{-3}	-4.22×10^{-2}	3.26×10^{-3}
34	-3.54×10^{-2}	-5.87×10^{-2}	2.37×10^{-3}
35	0	0	0
36	1.78×10^{-1}	2.14×10^{-1}	2.99×10^{-1}
37	-3.73×10^{-3}	-3.77×10^{-2}	6.62×10^{-3}
38	0	0	0
39	1.65×10^{-2}	-7.84×10^{-2}	1.63×10^{-2}

Figure 37. Concluded.

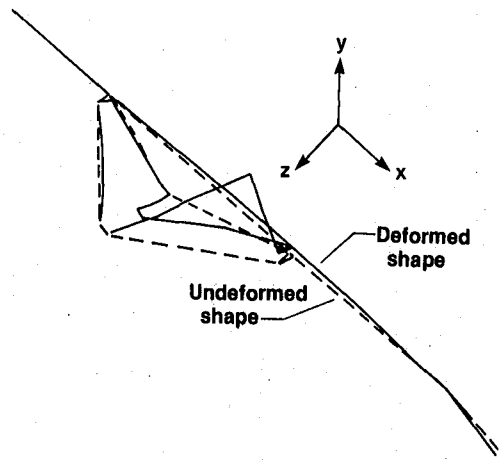

Point	Coefficient x	y	z
1	0	0	0
2	-1.19×10^{-4}	1.04×10^{-3}	-2.36×10^{-4}
3	-1.03×10^{-3}	4.16×10^{-3}	-2.58×10^{-3}
4	-3.77×10^{-3}	9.40×10^{-3}	-9.49×10^{-3}
5	-4.70×10^{-3}	1.06×10^{-2}	-1.17×10^{-2}
6	-1.55×10^{-2}	2.47×10^{-2}	-3.89×10^{-2}
7	-2.60×10^{-2}	3.57×10^{-2}	-6.49×10^{-2}
8	-2.94×10^{-2}	3.73×10^{-2}	-7.28×10^{-2}
9	-2.91×10^{-2}	3.67×10^{-2}	-7.19×10^{-2}
10	-2.49×10^{-2}	3.08×10^{-2}	-6.13×10^{-2}
11	-1.70×10^{-2}	2.06×10^{-2}	-4.08×10^{-2}

Figure 38. Fifth boom mode predicted by NASTRAN: frequency = 58.26 Hz.

12	-5.85×10^{-3}	6.97×10^{-3}	-1.22×10^{-2}
13	7.51×10^{-3}	-9.26×10^{-3}	2.21×10^{-2}
14	7.51×10^{-3}	-1.82×10^{-2}	4.37×10^{-2}
15	7.51×10^{-3}	-2.88×10^{-2}	6.93×10^{-2}
16	-5.23×10^{-2}	2.28×10^{-2}	-6.48×10^{-2}
17	-2.39×10^{-1}	-3.57×10^{-1}	-3.05×10^{-1}
18	-3.73×10^{-1}	-8.32×10^{-1}	-4.73×10^{-1}
19	-2.14×10^{-1}	-5.88×10^{-1}	-2.63×10^{-1}
20	4.72×10^{-6}	-1.04×10^{-2}	-7.36×10^{-4}
21	-8.12×10^{-5}	3.71×10^{-4}	-2.71×10^{-4}
22	6.59×10^{-3}	2.02×10^{-2}	-1.31×10^{-2}
23	4.28×10^{-3}	1.33×10^{-2}	-1.13×10^{-2}
24	6.87×10^{-3}	1.01×10^{-2}	-8.08×10^{-3}
25	1.69×10^{-2}	2.54×10^{-2}	-5.18×10^{-3}
26	-4.93×10^{-5}	5.25×10^{-3}	-2.22×10^{-4}
27	4.06×10^{-5}	3.63×10^{-2}	-7.95×10^{-4}
28	-1.39×10^{-1}	6.86×10^{-1}	5.99×10^{-2}
29	-3.22×10^{-1}	1.00	-5.12×10^{-2}
30	-2.40×10^{-1}	4.77×10^{-1}	-1.38×10^{-1}
31	-6.11×10^{-2}	2.67×10^{-2}	-8.52×10^{-2}
32	-2.92×10^{-2}	3.70×10^{-2}	-7.25×10^{-2}
33	-4.02×10^{-3}	1.00×10^{-2}	-1.04×10^{-2}
34	1.67×10^{-2}	2.65×10^{-2}	-3.06×10^{-3}
35	0	0	0
36	-6.20×10^{-2}	4.38×10^{-1}	6.65×10^{-2}
37	4.72×10^{-3}	1.61×10^{-2}	-9.23×10^{-3}
38	0	0	0
39	-1.13×10^{-1}	-3.48×10^{-1}	-1.45×10^{-1}

Figure 38. Concluded.

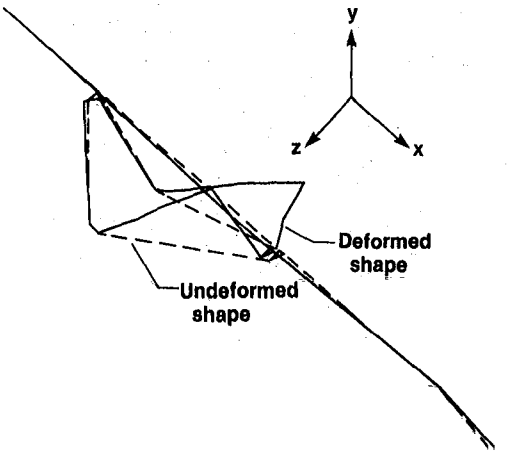

Point	Coefficient x	y	z
1	0	0	0
2	-6.24×10^{-4}	-4.71×10^{-3}	-1.29×10^{-3}
3	-2.66×10^{-3}	-1.66×10^{-2}	-6.34×10^{-3}
4	-6.89×10^{-3}	-3.27×10^{-2}	-1.68×10^{-2}
5	-8.15×10^{-3}	-3.64×10^{-2}	-1.99×10^{-2}
6	-2.18×10^{-2}	-6.60×10^{-2}	-5.26×10^{-2}
7	-3.27×10^{-2}	-8.30×10^{-2}	-8.06×10^{-2}
8	-3.59×10^{-2}	-8.24×10^{-2}	-8.75×10^{-2}
9	-3.55×10^{-2}	-8.11×10^{-2}	-8.63×10^{-2}
10	-3.09×10^{-2}	-7.01×10^{-2}	-7.44×10^{-2}
11	-2.20×10^{-2}	-5.06×10^{-2}	-5.16×10^{-2}

Figure 39. Sixth boom mode predicted by NASTRAN: frequency = 62.81 Hz.

12	-9.68×10^{-3}	-2.39×10^{-2}	-1.97×10^{-2}
13	5.52×10^{-3}	8.60×10^{-3}	1.92×10^{-2}
14	5.53×10^{-3}	3.16×10^{-2}	4.36×10^{-2}
15	5.53×10^{-3}	5.89×10^{-2}	7.28×10^{-2}
16	-4.53×10^{-2}	-8.34×10^{-2}	-8.60×10^{-2}
17	-1.73×10^{-2}	3.87×10^{-1}	-3.61×10^{-2}
18	7.34×10^{-2}	1.00	9.02×10^{-2}
19	1.09×10^{-1}	7.21×10^{-1}	1.37×10^{-1}
20	2.04×10^{-4}	2.60×10^{-2}	-7.41×10^{-4}
21	-1.42×10^{-4}	-2.48×10^{-3}	-5.53×10^{-4}
22	9.80×10^{-3}	-2.14×10^{-2}	-2.01×10^{-2}
23	7.35×10^{-3}	-2.77×10^{-2}	-1.96×10^{-2}
24	-1.29×10^{-2}	-3.39×10^{-2}	-1.30×10^{-2}
25	-1.33×10^{-2}	-2.90×10^{-2}	-8.27×10^{-3}
26	7.58×10^{-6}	-1.18×10^{-3}	-4.91×10^{-5}
27	-9.21×10^{-5}	2.49×10^{-2}	-4.05×10^{-4}
28	-1.31×10^{-1}	4.39×10^{-1}	-1.03×10^{-2}
29	-2.95×10^{-1}	6.18×10^{-1}	-1.40×10^{-1}
30	-2.03×10^{-1}	2.33×10^{-1}	-1.63×10^{-1}
31	-4.94×10^{-2}	-8.29×10^{-2}	-8.80×10^{-2}
32	-3.57×10^{-2}	-8.19×10^{-2}	-8.70×10^{-2}
33	-7.24×10^{-3}	-3.42×10^{-2}	-1.81×10^{-2}
34	-1.11×10^{-2}	-2.07×10^{-2}	-3.52×10^{-3}
35	0	0	0
36	-5.93×10^{-2}	2.86×10^{-1}	2.19×10^{-2}
37	5.28×10^{-3}	-1.52×10^{-2}	-1.12×10^{-2}
38	0	0	0
39	7.56×10^{-2}	4.51×10^{-1}	9.75×10^{-2}

Figure 39. Concluded.

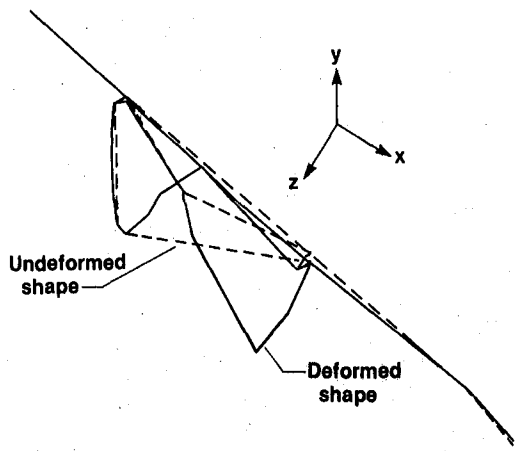

Point	Coefficient x	Coefficient y	Coefficient z
1	0	0	0
2	2.60×10^{-4}	-2.18×10^{-3}	-6.54×10^{-5}
3	1.10×10^{-3}	-8.02×10^{-3}	1.41×10^{-3}
4	3.46×10^{-3}	-1.65×10^{-2}	6.68×10^{-3}
5	4.25×10^{-3}	-1.85×10^{-2}	8.51×10^{-3}
6	1.35×10^{-2}	-3.64×10^{-2}	3.04×10^{-2}
7	2.22×10^{-2}	-4.64×10^{-2}	5.09×10^{-2}
8	2.53×10^{-2}	-4.29×10^{-2}	5.69×10^{-2}
9	2.51×10^{-2}	-4.15×10^{-2}	5.63×10^{-2}
10	2.27×10^{-2}	-3.33×10^{-2}	4.99×10^{-2}
11	1.77×10^{-2}	-2.26×10^{-2}	3.68×10^{-2}

Figure 40. Seventh boom mode predicted by NASTRAN: frequency = 73.85 Hz.

12	1.01×10^{-2}	-9.36×10^{-3}	1.75×10^{-2}
13	6.53×10^{-4}	5.93×10^{-3}	-6.93×10^{-3}
14	6.54×10^{-4}	9.76×10^{-3}	-2.25×10^{-2}
15	6.54×10^{-4}	1.43×10^{-2}	-4.11×10^{-2}
16	4.42×10^{-2}	-3.93×10^{-2}	5.56×10^{-2}
17	4.82×10^{-1}	-2.74×10^{-1}	6.00×10^{-1}
18	8.21×10^{-1}	-5.07×10^{-1}	1.00
19	3.85×10^{-1}	-3.24×10^{-1}	4.45×10^{-1}
20	6.40×10^{-5}	-5.02×10^{-2}	2.96×10^{-3}
21	6.80×10^{-5}	-1.09×10^{-3}	2.15×10^{-4}
22	-5.68×10^{-3}	-2.91×10^{-2}	1.12×10^{-2}
23	-3.01×10^{-3}	-2.17×10^{-2}	8.48×10^{-3}
24	-8.56×10^{-3}	-1.76×10^{-2}	4.08×10^{-3}
25	-2.16×10^{-2}	-3.55×10^{-2}	2.59×10^{-3}
26	5.09×10^{-5}	-5.92×10^{-3}	2.02×10^{-4}
27	-2.49×10^{-4}	2.89×10^{-2}	-8.68×10^{-4}
28	-3.06×10^{-1}	2.27×10^{-1}	-2.94×10^{-1}
29	-5.61×10^{-1}	3.39×10^{-1}	-5.53×10^{-1}
30	-2.30×10^{-1}	1.31×10^{-1}	-2.20×10^{-1}
31	4.68×10^{-2}	-3.96×10^{-2}	5.94×10^{-2}
32	2.53×10^{-2}	-4.22×10^{-2}	5.66×10^{-2}
33	3.68×10^{-3}	-1.74×10^{-2}	7.46×10^{-3}
34	-2.17×10^{-2}	-3.54×10^{-2}	2.05×10^{-3}
35	0	0	0
36	-1.52×10^{-1}	1.61×10^{-1}	-1.34×10^{-1}
37	-4.54×10^{-3}	-2.32×10^{-2}	8.69×10^{-3}
38	0	0	0
39	1.54×10^{-1}	-2.58×10^{-1}	1.88×10^{-1}

Figure 40. Concluded.

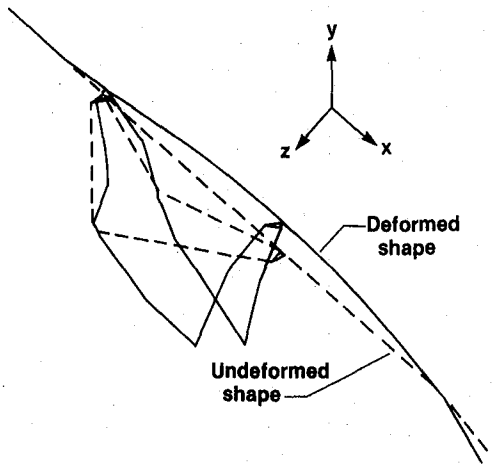

Point	Coefficient x	y	z
1	0	0	0
2	-2.08×10^{-3}	5.15×10^{-3}	-7.31×10^{-4}
3	-7.69×10^{-3}	1.95×10^{-2}	-1.08×10^{-2}
4	-2.11×10^{-2}	4.17×10^{-2}	-4.05×10^{-2}
5	-2.54×10^{-2}	4.74×10^{-2}	-5.03×10^{-2}
6	-7.40×10^{-2}	9.86×10^{-2}	-1.63×10^{-1}
7	-1.17×10^{-1}	1.29×10^{-1}	-2.64×10^{-1}
8	-1.35×10^{-1}	1.26×10^{-1}	-2.98×10^{-1}
9	-1.35×10^{-1}	1.24×10^{-1}	-2.97×10^{-1}
10	-1.27×10^{-1}	1.09×10^{-1}	-2.76×10^{-1}
11	-1.04×10^{-1}	8.45×10^{-2}	-2.16×10^{-1}

Figure 41. Eighth boom mode predicted by NASTRAN: frequency = 86.10 Hz.

12	-6.48×10^{-2}	4.86×10^{-2}	-1.15×10^{-1}
13	-1.23×10^{-2}	2.77×10^{-3}	2.04×10^{-2}
14	-1.23×10^{-2}	-2.60×10^{-2}	1.08×10^{-1}
15	-1.23×10^{-2}	-6.07×10^{-2}	2.15×10^{-1}
16	-1.84×10^{-1}	7.22×10^{-2}	-2.69×10^{-1}
17	2.69×10^{-1}	-1.43×10^{-1}	3.05×10^{-1}
18	8.44×10^{-1}	-3.29×10^{-1}	1.00
19	4.89×10^{-1}	-2.06×10^{-1}	5.61×10^{-1}
20	4.47×10^{-4}	-5.60×10^{-2}	2.53×10^{-3}
21	-3.91×10^{-4}	2.00×10^{-3}	-1.31×10^{-3}
22	3.05×10^{-2}	9.57×10^{-2}	-6.12×10^{-2}
23	1.71×10^{-2}	5.98×10^{-2}	-4.86×10^{-2}
24	2.74×10^{-2}	4.50×10^{-2}	-3.38×10^{-2}
25	8.63×10^{-2}	1.29×10^{-1}	-2.40×10^{-2}
26	-2.23×10^{-4}	2.51×10^{-2}	-1.03×10^{-3}
27	8.41×10^{-4}	-2.82×10^{-2}	1.02×10^{-4}
28	4.24×10^{-1}	-1.98×10^{-1}	4.31×10^{-1}
29	7.13×10^{-1}	-3.57×10^{-1}	6.94×10^{-1}
30	1.31×10^{-1}	-1.18×10^{-1}	4.89×10^{-2}
31	-2.31×10^{-1}	8.63×10^{-2}	-3.42×10^{-1}
32	-1.35×10^{-1}	1.25×10^{-1}	-2.97×10^{-1}
33	-2.23×10^{-2}	4.42×10^{-2}	-4.47×10^{-2}
34	8.92×10^{-2}	1.39×10^{-1}	-1.50×10^{-2}
35	0	0	0
36	2.14×10^{-1}	-1.31×10^{-1}	2.11×10^{-1}
37	2.25×10^{-2}	7.86×10^{-2}	-4.41×10^{-2}
38	0	0	0
39	2.10×10^{-1}	-1.96×10^{-1}	2.53×10^{-1}

Figure 41. Concluded.

1. Report No.	2. Government Accession No.	3. Recipient's Catalog No.
NASA TM-84914		

4. Title and Subtitle	5. Report Date
F-8 Refueling Boom Ground Vibration Test	January 1985
	6. Performing Organization Code
7. Author(s)	8. Performing Organization Report No.
Michael W. Kehoe	H-1194
	10. Work Unit No.
9. Performing Organization Name and Address NASA Ames Research Center Dryden Flight Research Facility P.O. Box 273 Edwards, California 93523	11. Contract or Grant No.
	13. Type of Report and Period Covered Technical Memorandum
12. Sponsoring Agency Name and Address National Aeronautics and Space Administration Washington, D.C. 20546	14. Sponsoring Agency Code RTOP 505-34-11

15. Supplementary Notes

16. Abstract

A ground vibration test was conducted on a simulated refueling boom mounted on an F-8 airplane. The ground vibration test was conducted to determine if the refueling boom modal frequencies were close to the airplane frequencies. The data presented in this report include modal frequencies, mode shape data, and structural damping coefficients.

17. Key Words (Suggested by Author(s))	18. Distribution Statement
Ground vibration test Vibration Modal analysis	Unclassified-Unlimited STAR category 05

19. Security Classif. (of this report)	20. Security Classif. (of this page)	21. No. of Pages	22. Price*
Unclassified	Unclassified	48	A03

For sale by the National Technical Information Service, Springfield, Virginia 22161.